Efficiently Computing First Passage Probabilities Under Metastable Equilibrium

Jackson Loper*

Data Science Institute, Columbia University, New York, NY, USA

Guangyao Zhou* and Stuart Geman

Division of Applied Mathematics, Brown University, Providence, RI, USA

(Dated: August 27, 2019)

A reversible stochastic differential equation is initialized at position x_0 – where will it go next? What is the probability it will reach one region before it reaches another region? We here propose an approach for estimating the probability that a given target, among many, will be the first to be reached by a reversible stochastic differential equation. We focus on the situation that it takes a long time to hit any target; in this case direct simulation of the hitting probabilities becomes prohibitively expensive. We turn this curse into a blessing; if the timescales are sufficiently long the system will reach metastable equilibrium before it hits any target. In this case we show that the hitting probabilities can be accurately approximated using only local simulations around each target, obviating the need for global simulations. Numerical experiments on idealized energy landscape show the estimates can be nearly as accurate as direct simulations and thousands of times faster to compute.

* These two authors contributed equally

Introduction

Reversible diffusions play a key role in a wide variety of physical systems. The folding of macromolecules into their native configurations is often posed as diffusions (either directly through simulations of atomic dynamics or indirectly through mesoscopic models [19, 21, 29]), the fluctuation of chemical species in solution can also be modeled as diffusions ("chemical Langevin equations" are one classic example of this approach [17, 30]), the motion of particles through membranes can be posed as a diffusion [18], and so-on. A full analytic understanding of these diffusions is usually impossible. However, it is sometimes possible to get accurate estimations of certain aspects of these diffusion systems.

In this paper we focus on estimating first-passage hitting probabilities for reversible diffusions: given an initial condition X_0 and two targets, A, B, what is the probability that we will hit target A first? The simplest way to estimate these hitting probabilities is by direct simulation of the diffusion. However, this simulation can be prohibitively computationally expensive, and many efforts have been made to understand diffusion without direct simulations, including frameworks such as kinetic transition networks (cf. [26, 32]), Markov State Models (cf. [11, 20, 27]), transition path sampling (cf. [7, 13]), transition interface sampling (cf. [31]), and transition path theory (cf. [15, 16]).

We focus particularly on the case that the first passage takes long enough that the system can reach a metastable equilibrium before either target is hit (we will make the idea of "metastable equilibrium" formally rigorous in Section II). In this case many approaches for accelerating simulation can fail [4, 25, 35]. Some authors take a pessimistic view on this subject: "If these processes are intrinsically slow, i.e. require an extensive sampling of state space, not much can be done to speed up their simulation without destroying the dynamics of the system" [12]. We here show an opposing viewpoint: processes in metastable equilibrium extensively sample the state-space but they are also much easier to analyze.

The "narrow escape problem" literature has already made great strides in understanding diffusions in a metastable equilibrium. This literature generally considers Brownian motion trapped in a set by reflecting boundaries and looks at the first passage times to asymptotically vanishing targets on the surface of the ball (cf. [10, 18]). This timing information usually enables estimation of the probability of hitting a particular target first. Techniques

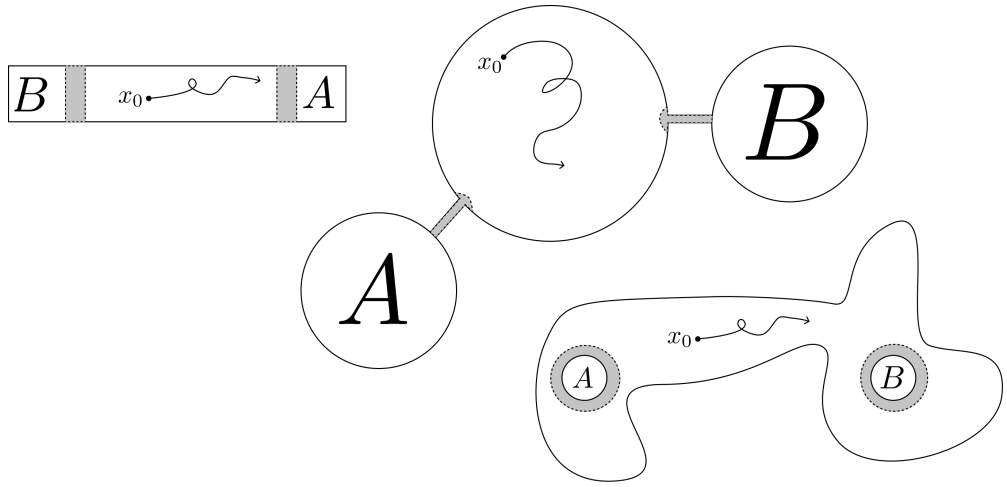

Figure 1. **First passage capacities allow efficient computation of hitting probabilities.** A reversible stochastic differential equation in an n-dimensional state-space is initialized at position x_0. What is the probability it will reach region A first before B? Subject to an "ϵ-flatness" condition, Theorem 1 shows that this probability can be approximated to within $\sqrt{2\epsilon}$ using only "first passage capacities." These capacities can be computed using local simulations in neighborhoods around the targets. Above we show several examples of this kind of problem. In each case, we can approximate first passage capacities using only local simulations performed in the gray areas.

such as matched asymptotics make it possible to obtain these timing formulas for many special cases [10].

We propose a set-capacity-based approach for estimating hitting probabilities when X reaches metastable equilibrium before it hits the targets. This capacity approach applies in high-dimensions, carries exact non-asymptotic error bounds, and can be applied to targets of any smooth shape on any smooth reversible diffusions. The key idea is to focus on type of set capacity, which we will refer to as "first-passage capacities." These capacities can be computed using only local simulations around the targets and can be used to accurately estimate the hitting probabilities. Figure 2 shows several examples. First-passage capacities allow analysis of a wider variety of problems than the extant narrow-escape results; however, these capacities are also less powerful insofar as they only estimate hitting probabilities and give no insights into timing.

In the following section (§II, "Preliminaries") we will introduce notation, make a formal condition for "metastable equilibrium," and define the first-passage capacities that are at the heart of this approach. In §III we show that these capacities can be used to accurately estimate first-passage probabilities as long as the metastable equilibrium condition holds; we also give an example where this condition is guaranteed. In §IV, we develop an approach

to computing the first passage capacities. In §V we look at the results of computational experiments on a five-dimensional diffusion.

Preliminaries

Let us first define our diffusion process. Our results are about a diffusion process X confined to an open bounded set $\Omega \subset \mathbb{R}^n$ with reflecting smooth boundary $\partial\Omega$. We assume X is driven by an n-dimensional standard Brownian motion W, i.e.

$$\mathrm{d}X_t = b(X_t)\mathrm{d}t + \sigma(X_t)\mathrm{d}W_t \tag{1}$$

where $b : \Omega \to \mathbb{R}^n$ and $\sigma : \Omega \to \mathbb{R}^{n\times n}$ are continuously differentiable vector-valued and matrix-valued functions. We further assume that $a(x) = \sigma(x)\sigma(x)^T$ is uniformly elliptic on Ω, i.e. the smallest eigenvalues of a are bounded away from zero. Let $\bar{\Omega}$ denote the closure of Ω (and in general let $\bar{S}$ denote the closure of any set $S \subset \bar{\Omega}$). For the precise definition of the reflected process, we adopt the framework developed by Lions and Sznitman[23]: Let $\mathfrak{n} = \mathfrak{n}(x)$ denote the outward normal of $\partial\Omega$ and $\nu : \partial\Omega \to \mathbb{R}^n$ a smooth vector field satisfying $\mathfrak{n}^T\nu \geq c > 0$, and assume that $x_0 \in \Omega$. Then there is a unique pathwise continuous and W-adapted strong Markov process $X_t \in \bar{\Omega}$, and (random) measure L, such that

$$X_t = x_0 + \int_0^t b(X_s)ds + \int_0^t \sigma(X_s)dW_s - \int_0^t \nu(X_s)L(ds) \tag{2}$$

and $L(\{t : \ X_t \notin \partial\Omega\}) = 0$. For convenience, we will refer to X by simply saying "the reflected diffusion process (1)." We further assume that X is a reversible process, with equilibrium distribution given by

$$\rho(dx) \doteq \frac{1}{Z}e^{-U(x)} \quad Z = \int_{x\in\Omega} e^{-U(x)}dx$$

where $U : \bar{\Omega} \to \mathbb{R}$ is continuously differentiable. As shown by Chen[8], to ensure that X is reversible it is sufficient that

$$\begin{aligned} b_i(x) &= \frac{1}{2}\sum_j \partial a_{ij}(x)/\partial x_j - \frac{1}{2}\sum_j a_{ij}(x)\partial U(x)/\partial x_j \\ \nu(x) &= a(x)\mathfrak{n}(x) \end{aligned} \tag{3}$$

where $a(x) = \sigma(x)\sigma(x)^T$ is uniformly elliptic. When the conditions in (3) are in force we will say that X satisfies the reversibility conditions relative to U. We assume these conditions throughout the paper.

The main goal of this paper is to estimate first passage hitting probabilities for X. We here give a formal definition for these hitting probabilities:

Definition 1. *(First passage hitting probabilities). Fix two disjoint sets $A, B \subset \Omega$. The first-passage hitting probability function $h_{A,B}(x)$ indicates the probability that the process X visits A before B if it is initialized at $X_0 = x$. Formally,*

$$h_{A,B}(x) \triangleq \mathbb{P}(X_{\tau_{A\cup B}} \in A | X_0 = x)$$

where $\tau_{A\cup B}$ indicates the first passage time to $A \cup B$, i.e. $\tau_{A\cup B} \triangleq \inf\{t \geqslant 0 : X_t \in A \cup B\}$. Throughout this paper we will use τ_S to denote the first passage time to a set S and $h_{S,S'}$ to denote the hitting probability function for targets S, S'.

It turns out that these hitting probabilities are much easier to estimate if the process reaches a metastable equilibrium before hitting either target. To make this idea rigorous, we develop a condition we can use to quantify the somewhat amorphous concept of metastable equilibrium:

Definition 2. *(The ε-flatness condition) A hitting probabiliy function $h_{A,B}(x)$ is said to be "ε-flat relative to M" whenever*

$$\sup_{x,y\in M} |h_{A,B}(x) - h_{A,B}(y)| < \varepsilon$$

To see how this condition is related to metastable equilibrium, consider a process X which achieves a metastable equilibrium in the region M before it hits A or B. In this case, the

process X will have "forgotten its starting position" within M by the time it achieves first passage. It follows that the hitting probability function $h_{A,B}$ (which indicates the hitting probability from each possible initial conditions) will be nearly constant over the region M. Thus, if the process X has a very large amount of time to mix inside M and thereby achieves a very well-mixed state, $h_{A,B}$ will be ε-flat with a very small constant. (Note however that $h_{A,B}$ may be ε-flat even if X is unlikely to achieve any kind of equilibrium; for example, if the target A is unreachable then we will always have $h_{A,B}(x) = 0$.)

The ε-flatness of $h_{A,B}$ is only a narrow view into the equilibrium of the process X. However it is exactly the view we need; the ε-flatness of $h_{A,B}$ gives us a way to quantify the extent of the equilibrium with respect to what we're interested in. As we shall see in Theorem 1, it is also exactly the condition we need to show that the hitting probabilities within M can be well-approximated using "first-passage capacities." These capacities are the last piece we must define:

Definition 3. *(Capacity) Let $S \subset \tilde{S} \subset \Omega$ be open sets and let X be a diffusion governed by the SDE in Equation (2) and satisfying the reversibility conditions in Equation (3). The first-passage capacity* $\mathrm{cap}(S, \tilde{S})$ *for X is defined as*

$$\mathrm{cap}(S, \tilde{S}) \triangleq \int_{\tilde{S} \setminus S} ||\sigma(x) \nabla h_{S, \tilde{S}^c}(x)||^2 e^{-U(x)} \mathrm{d}x$$

We refer the reader to Appendix A for more details on capacity and the related concept of Dirichlet form. Note that there are several related definitions of "capacity" in the probabilistic potential theory literature, all slightly different. Throughout this work, the term is used only in the sense of the above definition.

Main theoretical results

Our main theorem shows that the first-passage capacities gives accurate approximations of the hitting probabilities when the hitting probabilities are themselves ε-flat in a region outside a neighborhood of the targets.

Theorem 1. *Let $A \subset \tilde{A}, B \subset \tilde{B}$ be open sets and assume that $h_{A,B}(x)$ is ε-flat relative to $\Omega \setminus (\tilde{A} \cup \tilde{B})$. Then the first-passage probabilities are well-approximated by the first-passage*

capacities:

$$\sup_{x \notin \tilde{A}, \tilde{B}} \left| h_{A,B}(x) - \frac{\text{cap}(A, \tilde{A})}{\text{cap}(A, \tilde{A}) + \text{cap}(B, \tilde{B})} \right| \leqslant \varepsilon + \sqrt{\varepsilon/2}$$

We defer the proof to Appendix C. Note that the generalization to multiple targets is straightforward due to the additive property of capacities (Proposition 2 in Appendix A); if you have n targets and approximate the hitting probability to each by taking it to be proportional to the corresponding capacity, then all probabilities will be within $\varepsilon + \sqrt{\varepsilon/2}$ of the truth.

When does the ε-flatness condition hold? Speaking loosely, it will hold as long as X achieves a metastable equilibrium in M before hitting the targets; the first passage time must be long relative to the rate of ergodicity inside of M. Each diffusion may require a different method to prove this property.

To give the reader a flavor for how the ε-flatness condition may be proved, we will flesh out one example in detail. Let Ω denote any convex set with diameter 1 in $\mathbb{R}^n$, $n \geq 3$. We will be interested in two targets:

$$A \triangleq \mathcal{B}(x_A, r_A)$$
$$B \triangleq \mathcal{B}(x_B, r_B)$$

where $\mathcal{B}(x, r) \triangleq \{y : ||y - x|| < r\}$. Given an initial condition $X_0 \in \Omega \backslash (A \cup B)$, we are interested to know whether the dynamics carry the system into A or B first. The function $h_{A,B}(x)$ denotes the probability that X_t reaches A before reaching B, which depends on the starting configuration $X_0 = x$. Figure 2 may help visualize the setup.

We would like to be able to estimate $h_{A,B}$ using only local simulations in a local neighborhood around the targets. To this end, we define two sets around each target: $\dot{A} = \mathcal{B}(x_A, r_{\dot{A}})$ and $\tilde{A} = \mathcal{B}(x_A, r_{\tilde{A}})$ such that $r_A < r_{\dot{A}} < r_{\tilde{A}}$, and $\dot{B} = \mathcal{B}(x_B, r_{\dot{B}})$ and $\tilde{B} = \mathcal{B}(x_B, r_{\tilde{B}})$ such that $r_B < r_{\dot{B}} < r_{\tilde{B}}$. We assume that $\tilde{A}, \tilde{B}$ are completely enclosed inside of Ω. We also assume that $\nabla U(x) = 0$ for all $x \in \Omega \backslash (\dot{A} \cup \dot{B})$. Though U may be arbitrarily complicated on $\dot{A} \cup \dot{B}$, the hitting probabilities $h_{A,B}(x)$ converge uniformly over $x \in \Omega \backslash (\tilde{A} \cup \tilde{B})$ to a constant as the "action regions" $\dot{A}$ and $\dot{B}$ are made smaller. Moreover, if the dimension of the state-space is large, these action regions will always becomes small, because

Theorem 2. *Assume X is a diffusion governed by the example model described above. For*

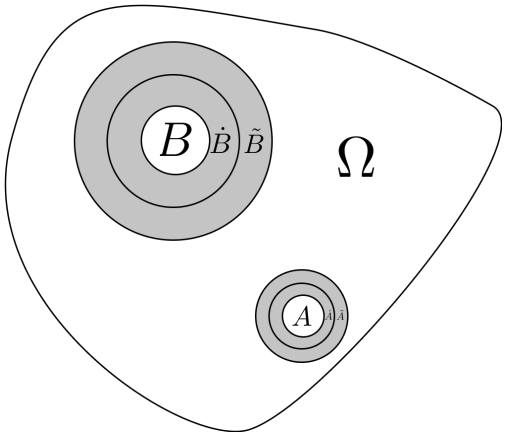

Figure 2. **A Toy Model.** We consider a toy example where the targets are nested balls and the energy is flat outside of $\dot{A} \cup \dot{B}$ (i.e. $\nabla U = 0$). If the targets are small enough or the dimension large enough then the probability of entering A before entering B is nearly independent of X_0, provided that X_0 is outside of $\tilde{A} \cup \tilde{B}$. This first-passage probability can thus be and can be well-approximated using first-passage capacities.

any fixed value of the dimension $n \geq 3$ and any $r_{\tilde{A}}, r_{\tilde{B}}, \varepsilon > 0$, there exists a constant $c = c(n, r_{\tilde{A}}, r_{\tilde{B}}, \varepsilon)$ such that if $r_{\dot{A}}, r_{\dot{B}} < c$ then $h_{A,B}(x)$ is ε-flat relative to $\Omega/(\tilde{A} \cup \tilde{B})$. Likewise, for any fixed values of $r_{\dot{A}}, r_{\tilde{A}}, r_{\dot{B}}, r_{\tilde{B}}, \varepsilon > 0$, there exists a constant $c = c(r_{\dot{A}}, r_{\tilde{A}}, r_{\dot{B}}, r_{\tilde{B}}, \varepsilon)$ such that if $n \geq c$ then $h_{A,B}(x)$ is ε-flat relative to $\Omega/(\tilde{A} \cup \tilde{B})$.

A proof can be found in Appendix B.

Capacity Estimation

For a class of stochastic systems, characterized by a separation of time scales such that the process of finding targets is slow compared to the process of exploring the regions away from the targets, we have reduced the estimation of first-passage probabilities to the evaluation, or approximation, of capacities. Generically, given the process defined in Equation (1), satisfying the reversibility conditions in (3) relative to a continuously differentiable energy U, our goal is to evaluate

$$\text{cap}(A, \tilde{A}) = \int_{\tilde{A} \setminus A} ||\sigma(x) \nabla h_{A, \tilde{A}^c}(x)||^2 e^{-U(x)} \mathrm{d}x \tag{4}$$

for a target A and neighborhood $\tilde{A}$.

The calculation is local, in that $\text{cap}(A, \tilde{A})$ depends only on the behavior of U on $\tilde{A} \setminus A$,

but it is not uncomplicated. We will propose here a Monte Carlo approach to evaluating the integral, made up of a combination of analytic reductions and highly orchestrated random walks. Inevitably, the effectiveness, or even feasibility, of the approach will depend on the particulars of the stochastic system, (1).

We begin by replacing the volume integral in (4) with a surface integral:

Proposition 1. *For any regions G and $\tilde{G}$ having smooth boundaries and such that $A \subset G \subset \tilde{G} \subset \tilde{A}$, $\mathrm{cap}(A, \tilde{A},)$ can be expressed as a flux leaving $\tilde{G}\backslash G$:*

$$\mathrm{cap}(A, \tilde{A}) = \int_{\partial(\tilde{G}\backslash G)} h_{A,\tilde{A}^c}(x)\mathfrak{n}(x)^T a(x)\nabla h_{G,\tilde{G}^c}(x)e^{-U(x)}\mathscr{H}(dx) \tag{5}$$

where $a(x) = \sigma(x)\sigma(x)^T$ is the diffusion matrix, $\mathscr{H}(dx)$ is the $(n-1)$-dimensional Hausdorff measure, and $\mathfrak{n}$ represents the outward-facing (relative to the set $\tilde{G}\backslash G$) normal vector on $\partial(\tilde{G}\backslash G)$.

The proof is in Appendix D.

There is a great deal of freedom in choosing G and $\tilde{G}$; the idea is to choose them so as to make the surface integrals as simple as possible. Before pursuing this, we mention that there are many other ways to reduce the volume integral (4) to a flux integral, some of which might make more sense than (5) for a particular problem. Specifically, by a corollary of Proposition (1), $\mathrm{cap}(A, \tilde{A})$ can be written as the flux of a different field, but this time through a single surface (see Appendix D):

Corollary 1. *For any region S having smooth boundary ∂S, and such that $A \subset S \subset \tilde{A}$, $\mathrm{cap}(A, \tilde{A},)$ can be expressed as a flux leaving S:*

$$\mathrm{cap}(A, \tilde{A}) = \int_{\partial S} \mathfrak{n}(x)^T a(x)\nabla h_{A,\tilde{A}^c}(x)e^{-U(x)}\mathscr{H}(dx) \tag{6}$$

where a and $\mathscr{H}(dx)$ are as defined in the Proposition, and $\mathfrak{n}$ is the outward-facing normal on ∂S.

The possible advantage is that there is only one surface and the integrand involves only one first-passage probability function, $h_{A,\tilde{A}^c}(x)$, instead of two. The possible disadvantage is the need to estimate $\nabla h_{A,\tilde{A}^c}$ on S, which is harder than estimating $h_{A,\tilde{A}^c}$. As we will see shortly,

judicious choices for G and $\tilde{G}$ can mitigate, and in some cases even eliminate, the need to estimate gradients of first-passage probabilities.

Returning to the representation in (5), there are two surface integrals, each of which can be viewed as an expectation, as follows: Define a probability measure on ∂G by

$$\mathscr{P}(dx) \doteq \frac{1}{Z} e^{-U(x)} \mathscr{H}(dx) \text{ where } Z = \int_{\partial G} e^{-U(x)} \mathscr{H}(dx)$$

and define $\tilde{\mathscr{P}}(dx)$ and $\tilde{Z}$ analogously, but on $\partial \tilde{G}$ rather than ∂G. Then

$$\begin{aligned} \text{cap}(A, \tilde{A}) &= \int_{\partial \tilde{G}} h_{A,\tilde{A}^c} \mathfrak{n}^T a \nabla h_{G,\tilde{G}^c} e^{-U} \mathscr{H}(dx) - \int_{\partial G} h_{A,\tilde{A}^c} \mathfrak{n}^T a \nabla h_{G,\tilde{G}^c} e^{-U} \mathscr{H}(dx) \\ &= Z \int_{\partial \tilde{G}} h_{A,\tilde{A}^c} \mathfrak{n}^T a \nabla h_{G,\tilde{G}^c} \tilde{\mathscr{P}}(dx) - Z \int_{\partial G} h_{A,\tilde{A}^c} \mathfrak{n}^T a \nabla h_{G,\tilde{G}^c} \mathscr{P}(dx) \end{aligned} \tag{7}$$

where, in these integrals, the normal, $\mathfrak{n}$, points outward from *both* G and $\tilde{G}$. If now $y_1, y_2, \ldots, y_m \sim \text{iid } \mathscr{P}(dx)$, then

$$\frac{1}{m} \sum_{i=1}^{m} h_{A,\tilde{A}^c}(y_i) \mathfrak{n}^T(y_i) a(y_i) \nabla h_{G,\tilde{G}^c}(y_i) \overset{m\to\infty}{\longrightarrow} \int_{\partial G} h_{A,\tilde{A}^c} \mathfrak{n}^T a \nabla h_{G,\tilde{G}^c} \mathscr{P}(dx)$$

$$\text{and} \qquad \frac{1}{m} \sum_{i=1}^{m} e^{U(y_i)} \overset{m\to\infty}{\longrightarrow} \int_{\partial G} e^U \mathscr{P}(dx) = \frac{|\partial G|}{Z}$$

where $|\partial G|$ is the surface area of G. Putting these together, we get the large n approximation

$$Z \int_{\partial G} h_{A,\tilde{A}^c} \mathfrak{n}^T a \nabla h_{G,\tilde{G}^c} \mathscr{P}(dx) \approx |\partial G| \frac{\sum_{i=1}^m h_{A,\tilde{A}^c}(y_i) \mathfrak{n}^T(y_i) a(y_i) \nabla h_{G,\tilde{G}^c}(y_i)}{\sum_{i=1}^m e^{U(y_i)}}$$

If we now extend all of this to $\partial \tilde{G}$, with $\tilde{y}_1, \tilde{y}_2, \ldots, \tilde{y}_n \sim \text{iid } \tilde{\mathscr{P}}(dx)$, and put the approximations into (7), then for large n and m

$$\begin{aligned} \text{cap}(A, \tilde{A}) \approx\ & |\partial \tilde{G}| \frac{\sum_{i=1}^n h_{A,\tilde{A}^c}(\tilde{y}_i) \mathfrak{n}^T(\tilde{y}_i) a(\tilde{y}_i) \nabla h_{G,\tilde{G}^c}(\tilde{y}_i)}{\sum_{i=1}^n e^{U(\tilde{y}_i)}} \\ & - |\partial G| \frac{\sum_{i=1}^m h_{A,\tilde{A}^c}(y_i) \mathfrak{n}^T(y_i) a(y_i) \nabla h_{G,\tilde{G}^c}(y_i)}{\sum_{i=1}^m e^{U(y_i)}} \end{aligned} \tag{8}$$

To make this useful, we will need to choose G and $\tilde{G}$ so that (i) we can readily sample from $\mathscr{P}(dx)$ and $\tilde{\mathscr{P}}(dx)$; (ii) the surface areas $|\partial G|$ and $|\partial \tilde{G}|$ can be well approximated;

(iii) the first-passage probability $h_{A,\tilde{A}^c}$ can be well approximated on G and $\tilde{G}$; and (iv) the gradient $\nabla h_{G,\tilde{G}^c}$ can also be well approximated on G and $\tilde{G}$. The first two of these challenges lend themselves to more-or-less routine, though not necessarily easy methods, including importance and rejection sampling. Of course we're free to choose G and $\tilde{G}$ to make (i) and (ii) as easy as possible.

As for approximating first-passage probabilities and their gradients, broadly speaking there are two approaches. It is well known that first-passage probabilities satisfy an elliptic PDE related to the infinitesimal generator—see Appendix A, Equation (A1)—and we could therefore choose from a selection of numerical solvers. One drawback with this approach is that numerical PDE methods are famously difficult to employ successfully in high dimensions ("curse of dimensionality"). Here, in a different direction, we exploit the connection between first-passage probabilities and the underlying random walk in order to develop Monte Carlo tools suitable for estimating both $h_{A,\tilde{A}^c}$ and $\nabla h_{G,\tilde{G}^c}$ on the surfaces ∂G and $\partial\tilde{G}$. These tools are based on what we will call the "shell method," which we describe briefly in the following paragraphs and in full detail in Appendix F.

Generically, given two simply-connected regions R and $\tilde{R}$, with $R \subset \tilde{R}$, and a set S such that $R \subset S \subset \tilde{R}$, we seek an approximation to the function $h_{R,\tilde{R}^c}$ on the surface ∂S. In principle, we could begin with a fine-grained partitioning of ∂S into simply-connected "cells," and for each cell run the diffusion X_t many times, recording whether or not the path first exits $\partial(\tilde{R}\backslash R)$ at ∂R. The fraction of paths that first exit at ∂R constitutes an estimate of $h_{R,\tilde{R}^c}(x)$ for any x in the current cell. But this is wasteful and likely infeasible in all but the simplest of settings. Much of the waste stems from the fact that the ensemble of all paths generated from all cells will likely include many near collisions of paths scattered throughout $\partial(\tilde{R}\backslash R)$. An alternative, divide-and-conquer approach, is to introduce multiple sets, $S_0, S_1, \ldots, S_n$ such that

$$R = S_0 \subset \cdots \subset S_{m-1} \subset S_m = S \subset S_{m+1} \subset \cdots \subset S_n = \tilde{R}$$

and use sample paths from X, *locally*, to estimate the transition probability matrices from each cell within each "shell" ∂S_k to each cell of its neighboring shells, ∂S_{k-1} and ∂S_{k+1}. Equipped with these transition matrices, the first-passage probability for a given $x \in S$ is computed algebraically, without further approximation.

S must have been chosen not only to satisfy $R \subset S \subset \tilde{R}$ but also in such a way as to make it feasible to sample from ∂S under the probability measure $\frac{1}{Z}e^{-U}\mathscr{H}(dx)$. After that, S_k $k = 1, \ldots, n-1$ are chosen so that the shells nest and are in close proximity; the hitting times starting from a sample in ∂S_k and ending at $\partial S_{k-1} \cup \partial S_{k+1}$ must be short enough to encourage many repeated runs. The output is a set of samples, $z_1, \ldots, z_N \sim \frac{1}{Z}e^{-U}\mathscr{H}(dx)$ on ∂S together with the approximate value of $h_{R,\tilde{R}^c}(x)$ at each sample $x = z_i$. (In fact, though the main purpose is to estimate $h_{R,\tilde{R}^c}$ on ∂S, a byproduct is a sample from $\frac{1}{Z}e^{-U}\mathscr{H}(dx)$ on all of the shells ∂S_k, along with an estimate of $h_{R,\tilde{R}^c}$ at every sample.) With the choice of A for R and $\tilde{A}$ for $\tilde{R}$, the algorithm becomes directly applicable to the estimation of $h_{A,\tilde{A}^c}$ on ∂G and $\partial\tilde{G}$, taking $S = G$ in the former case and $S = \tilde{G}$ in the latter.

The shell method is closely related to milestoning[2, 5, 34] and Markov state models[11, 20, 27], though more tailored to the problem at hand. In particular, our interest here is in computing the first-passage probabilities rather than in approximating the underlying process. Also, the discretizations of the shells are *adaptive*, in that they are based on clusters that are derived from an ensemble of samples, as opposed to being crafted for a particular landscape. See Appendix F.

As for the required gradients, these are generally harder to estimate. Nevertheless, for the particular gradient $\nabla h_{G,\tilde{G}^c}$, the problem is substantially mitigated by noting that we are only interested in its evaluation on ∂G and $\partial\tilde{G}$, each of which is a level set of $h_{G,\tilde{G}^c}$ ($h_{G,\tilde{G}^c} = 1$ on G and 0 on $\tilde{G}$). Consequently, on each surface the gradient is in the normal direction and we need only estimate its magnitude. And for this purpose it is enough to know the values of $h_{G,\tilde{G}^c}$ on a surface close to G and interior to $\tilde{G}\backslash G$ (for estimating $\nabla h_{G,\tilde{G}^c}$ on G) and on another surface close to $\tilde{G}$ and also interior to $\tilde{G}\backslash G$ (for estimating $\nabla h_{G,\tilde{G}^c}$ on $\tilde{G}$). Two such surfaces would be ∂S_1 and ∂S_{n-1}, were we to apply the shell method with $R = G$ and $\tilde{R} = \tilde{G}$, since, as already noted, a byproduct of the method is an estimate of $h_{R,\tilde{R}^c}$ on all of the shells. Alternatively, in the interest of better accuracy, the method could be run twice, once with $S = S_1$, a well-chosen outer approximation of G, and then again with $S = S_{n-1}$, a well-chosen inner approximation of $\tilde{G}$.

Numerical Experiments[1]

We experimented with the two-target system discussed in §I and depicted in Figure 2, with $n = 5$ dimensions and the particular targets $A = \mathcal{B}(x_A, r_A)$, where $x_A = (0.5, 0.6, 0.0, 0, 0, 0.0)$ and $r_A = 0.02$, and $B = \mathcal{B}(x_B, r_B)$, where $x_B = (-0.7, 0.0, 0.0, 0, 0, 0.0)$ and $r_B = 0.04$. The configuration space is the unit ball centered at the origin, $\Omega = \mathcal{B}(0, 1)$. The goal is to estimate $h_{A,B}(x)$, the probability that A is visited before B, using only the behavior of U in the vicinity of the targets, provided that x, the starting configuration, is sufficiently far from $A \cup B$. The entropic barrier is idealized by assuming that $\nabla U(x) = 0$ outside of $\dot{A} = \mathcal{B}(x_{\dot{A}}, r_{\dot{A}})$ and $\dot{B} = \mathcal{B}(x_{\dot{B}}, r_{\dot{B}})$ and "sufficiently far away" means outside of $\tilde{A} \cup \tilde{B}$, where $\tilde{A} = \mathcal{B}(x_{\tilde{A}}, r_{\tilde{A}})$ and $\tilde{B} = \mathcal{B}(x_{\tilde{B}}, r_{\tilde{B}})$. The concentric neighborhoods around the targets are supposed to satisfy $A \subset \dot{A} \subset \tilde{A}$ and $B \subset \dot{B} \subset \tilde{B}$, which was enforced in our experiments by the choices $r_{\dot{A}} = 0.05$, $r_{\tilde{A}} = 0.1$, $r_{\dot{B}} = 0.075$, and $r_{\tilde{B}} = 0.15$. Our experiments test the overall approximation to $h_{A,B}$ developed in §III-IV as well as each of the three components, separately: ϵ-flatness, the role of capacities, and the methodology developed for estimating capacities.

The experimental setup is sufficiently simple to allow exhaustive simulation for approximating ground truth. In each experiment, we compare the results of using the approximations developed here to the results from an ensemble of first-passage events simulated by simply running the diffusion 2,000 times at each of 100 randomly chosen points in $\Omega \backslash (\tilde{A}, \tilde{B})$. There are two sets of experiments: In the first (a kind of "sanity check"), the potential U is flat everywhere outside of the targets A and B, in other words, the diffusion is Brownian motion. In the second, there are complex landscapes in the vicinities of the targets, i.e. within $\dot{A}$ and $\dot{B}$.

Both Theorems, 2 and 1, are in force, and hence the first-passage probability $h_{A,B}(x)$, on $\Omega \backslash (\tilde{A}, \tilde{B})$, is approximately a constant, and the value depends only on the two local capacities $\mathrm{cap}(A, \tilde{A})$ and $\mathrm{cap}(B, \tilde{B})$:

$$h_{A,B}(x) \approx \frac{\mathrm{cap}(A, \tilde{A})}{\mathrm{cap}(A, \tilde{A}) + \mathrm{cap}(B, \tilde{B})}$$

[2]All the experimental results can be reproduced or easily modified from open-source code, which can found, along with detailed instructions, at `https://github.com/StannisZhou/entropic_barrier`.

We need to compute, or approximate, $\text{cap}(A, \tilde{A})$ and $\text{cap}(B, \tilde{B})$. Will will work through the details for $\text{cap}(A, \tilde{A})$, but the identical considerations apply to $\text{cap}(B, \tilde{B})$. We start with the flux representation established in the Proposition, and the numerical approximation from Equation (8), which reduces the problem to selecting G and $\tilde{G}$ and then applying the shell method, as described in §IV. In the current setup, good choices for G and $\tilde{G}$ are $G = \dot{A}$ and $\tilde{G} = \tilde{A}$, as can be seen from the following observations:

1. Recall that $h_{A,\tilde{A}^c}(x)$ is the probability of first exiting $\tilde{A} \backslash A$ at ∂A rather than at $\partial \tilde{A}$, given that the process started at x. Consequently $h_{A,\tilde{A}^c}(x) = 0$ for all $x \in \partial \tilde{A}$, and hence also on $\partial \tilde{G}$. Hence, with reference to Equation (8), we need only consider the flux approximation on ∂G:

$$\text{cap}(A, \tilde{A}) \approx -|\partial G| \frac{\sum_{i=1}^{m} h_{A,\tilde{A}^c}(y_i) \mathfrak{n}(y_i) \cdot \nabla h_{G,\tilde{G}^c}(y_i)}{\sum_{i=1}^{m} e^{U(y_i)}} \tag{9}$$

   where $y_1, \ldots, y_m$ are independent samples from $\mathscr{P}(dx) = \frac{1}{Z} e^{-U} \mathscr{H}(dx)$ on ∂G, $\mathfrak{n}(x)$ faces outward from G, and compared to (8), we have used the fact that in the current setup $a(x)$ is the identity I.

2. The surface area $|\partial G|$ is just the area of the 4-sphere (in five dimensions), with radius $r_{\dot{A}}$:

$$|\partial G| = \frac{2\pi^{\frac{5}{2}}}{\Gamma(\frac{5}{2})} r_{\dot{A}}^4$$

3. Furthermore, since $\nabla U(x) = 0$ on $\Omega \backslash (\dot{A} \cup \dot{B})$ and the diffusion is unchanged by a constant shift of the potential, we can assume that $U(x) = 0$ on $\Omega \backslash (\dot{A} \cup \dot{B})$. Since $G = \dot{A}$ and since U is continuous, $U(x) = 0$ for all $x \in \partial G$. Hence $\sum_{i=1}^{m} e^{U(y_i)} = m$.

4. Since U is flat on $\tilde{G} \backslash G$, the first-passage function $h_{G,\tilde{G}^c}$ is that of a standard Brownian motion between two concentric spheres. The PDE in Equation (A1) of Appendix A reduces to an instance of Laplace's equation, with analytic solution[33]

$$h_{G,\tilde{G}^c}(x) = \frac{1}{r_{\dot{A}}^{-3} - r_{\tilde{A}}^{-3}} \|x - x_A\|^{-3} - \frac{r_{\tilde{A}}^{-3}}{r_{\dot{A}}^{-3} - r_{\tilde{A}}^{-3}}$$

from which the gradient is found to be

$$\nabla h_{G,\tilde{G}^c}(x) = \frac{-3}{r_{\dot{A}}^{-3} - r_{\tilde{A}}^{-3}} \|x - x_A\|^{-4} \frac{x - x_A}{\|x - x_A\|} = \frac{-3}{r_{\dot{A}}^{-3} - r_{\tilde{A}}^{-3}} \|x - x_A\|^{-4} \frac{x - x_A}{\|x - x_A\|}$$

And since $\|x - x_A\| = r_{\dot{A}}$ and $\frac{x-x_A}{\|x-x_A\|} = \mathfrak{n}(x)$,

$$\mathfrak{n}(x) \cdot \nabla h_{G,\tilde{G}^c}(x) = \frac{-3}{r_{\dot{A}}^4 (r_{\dot{A}}^{-3} - r_{\tilde{A}}^{-3})}$$

5. It remains to choose a sample $y_1, \ldots, y_m$ from $\mathscr{P}(dx)$ on G, and estimates of the accompanying values of $h_{A,\tilde{A}^c}(y_i),\ i = 1, \ldots, m$. Here, the shell method (Appendix F) can be used, with $R = A$, $\tilde{R} = \tilde{A}$, and $S = G$, resulting in the desired samples $y_1, \ldots, y_m$ and estimates of $h_{A,\tilde{A}^c}(y_1), \ldots, h_{A,\tilde{A}^c}(y_m)$, say $u_1, \ldots, u_m$.

Putting together the pieces, the approximation in (9) becomes

$$\mathrm{cap}(A, \tilde{A}) \approx \frac{6\pi^{\frac{5}{2}}}{\Gamma(\frac{5}{2})(r_{\dot{A}}^{-3} - r_{\tilde{A}}^{-3})} \frac{1}{m} \sum_{i=1}^{m} u_i \tag{10}$$

The approximation we used for $\mathrm{cap}(B, \tilde{B})$ is the same, but with the substitutions $A \to B$ and $\tilde{A} \to \tilde{B}$.

Brownian Diffusion

The first set of experiments test the approach in the simplest possible case: there is no gradient in U anywhere outside of the targets. Even though the resulting diffusion is just a standard Brownian motion, there are few symmetries in the configuration space and hence still no closed-form solution for the first-passage probabilities. There is however a large entropic barrier and an opportunity to dissect and test separately each component of the the overall approximation.

Are first-passage probabilities approximately constant outside of $\tilde{\boldsymbol{A}} \cup \tilde{\boldsymbol{B}}$?

Is it true that in regions with golf-course potentials, the hitting probability is approximately constant over initial conditions that are modestly far away from the targets? In other words, is $h_{A,B}$ ε-flat on $\Omega \backslash (\tilde{A} \cup \tilde{B})$? Theorem 2 shows that this must hold in the limiting regime of small r_A, r_B or large n, but it is not obvious whether the parameters of the current model lie in this regime.

We ran 2,000 diffusion simulations at each of 100 randomly selected initial conditions in the region $\mathcal{B}(0,1) \setminus (\tilde{A} \cup \tilde{B})$, yielding 100 well-estimated probabilities of hitting A before B. A histogram of these probabilities can be be found in panel (a) of Figure 3. The observations fall in a fairly narrow window, $[0.0820, 0.1185]$, suggesting that h is indeed ε-flat, with $\varepsilon \approx 0.0365$. In addition, the empirical distribution is quite peaked.

Are first-passage probabilities proportional to capacity?

According to Theorem 1, in light of the ε-flatness of $h_{A,B}$ with respect to $\Omega \backslash (\tilde{A} \cup \tilde{B})$, $h_{A,B}(x)$ should be well approximated by

$$p_A \doteq \frac{\text{cap}(A, \tilde{A})}{\text{cap}(A, \tilde{A}) + \text{cap}(B, \tilde{B})} \tag{11}$$

for $x \in \mathcal{B}(0,1) \setminus (\tilde{A} \cup \tilde{B})$. In the current experiment, with $\nabla U = 0$ on $\tilde{A} \backslash A$ and $\tilde{B} \backslash B$, the capacities can be computed analytically, e.g. from Corollary 1, with $S = A$ and $S = B$:

$$\text{cap}(A, \tilde{A}) = \frac{6\pi^{\frac{5}{2}}}{\Gamma(\frac{5}{2})(r_A^{-3} - r_{\tilde{A}}^{-3})} \qquad \text{cap}(B, \tilde{B}) = \frac{6\pi^{\frac{5}{2}}}{\Gamma(\frac{5}{2})(r_B^{-3} - r_{\tilde{B}}^{-3})} \tag{12}$$

and hence

$$p_A = \frac{\frac{1}{r_A^{-3} - r_{\tilde{A}}^{-3}}}{\frac{1}{r_A^{-3} - r_{\tilde{A}}^{-3}} + \frac{1}{r_B^{-3} - r_{\tilde{B}}^{-3}}} \approx 0.1100$$

This probability is within 2% of the average found by direct simulations, which was 0.0975.

Accuracy of the shell method.

Lastly, we check the accuracy of the capacity estimation algorithm that we call the shell method. Here, the exact values are available from the formulas in (12): $\text{cap}(A, \tilde{A}) = 0.000637$ and $\text{cap}(B, \tilde{B}) = 0.005151$. The approximate values come from two applications of (10), which produced 0.000591 and 0.004827, respectively.[3]

Had we used the estimated capacities instead of the actual capacities for computing p_A from Equation (11) the approximation of the first-passage probability, given $x \in \mathcal{B}(0,1) \setminus (\tilde{A} \cup \tilde{B})$, would have been 0.1091 instead of 0.1100.

In summary, all three components of the approach performed well in the Brownian motion test case.

[3]With reference to Appendix F, the following parameters were used to implement the shell method: $m = 2, n = 4, N_p = 100, N_b = 3, N_s = 1000$, and a time-step of 10^{-7}.

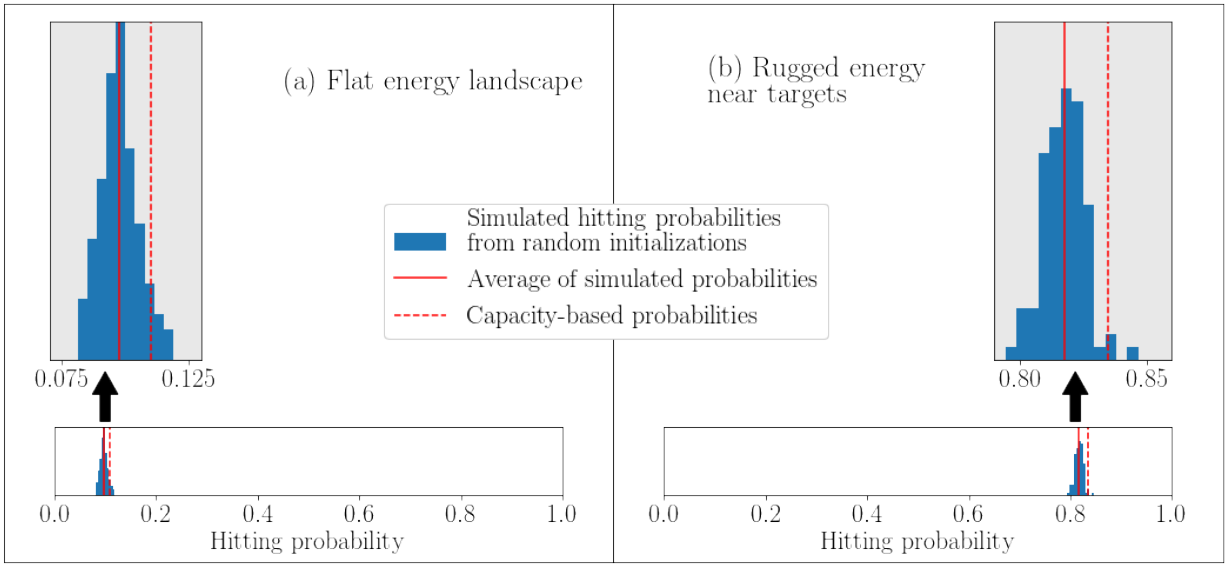

Figure 3. **Hitting probabilities: direct simulations vs. evaluation of local capacities.** Local capacities can accurately answer the question "where will we go next?" We start by designating two targets, A and B. For any given initial condition, the task is to determine the probability that the diffusion will hit A first. We study this question in the context of two different energy landscapes. In panel (a), we study the simplest possible case, where we have a flat energy landscape and the diffusion is simply a Brownian motion. In panel (b), we consider the case that the energy landscape becomes complicated near the targets. In both cases we consider 100 random initial locations which are modestly far away from either target. For each initial location, we conduct 2000 simulations to estimate the probability of hitting target A first. For both energy landscapes we see that the hitting probability is approximately constant for initial conditions which are modestly far away from the targets. Furthermore, the value of this constant is very nearly proportional to the ratio of the local capacities. In summary, in these simulations first-passage probabilities are accurately estimated using only local simulations around the targets, and do not require any computations that involve the large space around A and B.

Nontrivial Landscape

We performed the same tests, but with a complex energy landscape in the neighborhoods of the targets, i.e. on $\dot{A}\backslash A$ and $\dot{B}\backslash B$. The details of the specification can be found in Appendix G.

Are first-passage probabilities approximately constant outside of $\tilde{\boldsymbol{A}} \cup \tilde{\boldsymbol{B}}$?

Following the same procedure used in §V A 1 we tested for the near-constancy of $h_{A,B}$ on $\Omega\backslash(\tilde{A} \cup \tilde{B})$. The results are illustrated in Figure 3, panel (b). For each of the 100 initial conditions, the probability of first-passage at A fell in the interval $[0.7985, 0.8460]$, consistent with the conclusions of Theorem 2.

Are first-passage probabilities proportional to capacity?

In the previous experiments we were able to compute the capacities in closed form, and use p_A, from Equation (11), to directly verify the conclusion of Theorem 1. This is not possible in the current experiments. We are forced instead to use the estimated capacities, from which we obtained the estimate $p_A \approx 0.8360$, which is within 2% of 0.8175,[4] the average found by direct simulations.

Notable in these results is the fact that the larger target, B, is substantially less likely than A to be visited first. Evidently, the energy in $\dot{B}\backslash B$, the region surrounding B, introduces a significant barrier to the diffusion process, at least in comparison to the energy surrounding A. Keep in mind that the process here is identical to the one in the previous experiments, i.e. Brownian motion, for so long as the process remains outside of $\dot{A} \cup \dot{B}$, and that in those experiments the first-passage occurred at B approximately ten times more often than at A. Evidently, the process is much more likely to exit $\dot{B}\backslash B$ at $\partial\dot{B}$ than at ∂B, at least in comparison to the dynamics in $\dot{A}\backslash A$. These observations serve to further illustrate the role of local capacities and the importance of their accurate approximation.

Accuracy of the shell method.

As already remarked, the nontrivial energy landscape precludes a direct assessment of the accuracy of the capacity estimation algorithm. It is not possible to obtain exact values for the capacity. Therefore, we cannot directly test whether our algorithm is accurately estimating the capacities. However, the good agreement between the estimated value of p_A and the results of straightforward simulation constitute indirect evidence supporting the approximations, and the accuracy of the shell method in particular.

Concerning computational efficiency, it is difficult to make a direct comparison between the capacity-estimation approach and straightforward simulation. There are many parameters and, besides, run times will depend on the dimension and details of the energies, possibly affecting the two approaches differently. In our experiments, for direct simulations we used the "walk-on-spheres" method to simulate trajectories in the flat region,[6] JIT compilation to remove loop overhead, multi-CPU parallelization, and the coarsest time step that yielded accurate results. As for capacity estimation, we made no effort to adjust the number of samples or the discretization parameters. Under these conditions, a single run of the direct

[4]Using the following parameters (Appendix F): $m = 2$, $N_p = 3000$, $N_b = 5$, $N_s = 1000$, with time-step 10^{-6}. For target A we used $n = 4$ and for the larger target B we used $n = 5$.

simulation took about as long as estimating the two capacities.

Assume that $h_{A,B}(x)$ is ε-flat relative to $\Omega\backslash(\tilde{A} \cup \tilde{B})$. Both methods suffer if ε is large: direct simulation because it will depend on the initial condition, which is unknowable in any realistic experiment, and capacity estimation because the capacity ratio has a built-in error (Theorem 1) that depends on ε. If we assume that ε is negligible, then for a fixed $x \in \Omega\backslash(\tilde{A} \cup \tilde{B})$ we can more-or-less directly compare the standard deviations of the capacity-based estimation of $p \doteq h_{A,B}(x)$ via the shell method to direct simulation via repeated-samples. For example, under the specific (albeit idealized) circumstances of the experiments in §V A, about how many direct-simulation samples would be needed to attain a confidence interval for p of comparable width as from a single sample using capacity estimation by the shell method? The binomial estimator from n direct samples has standard deviation $\sqrt{\frac{p(1-p)}{n}}$, which we can compare to the empirical standard deviation, $\hat{\sigma} \approx 0.006$, from 100 runs of the shell method estimating p. Recall from §V A that $p \approx 0.1100$, in which case approximately $n = 2,700$ runs of direct simulation would be needed to get a comparable confidence interval. Bear in mind that a single run of the shell method requires about as much time as a single run of direct diffusion. It would appear, then, that capacity-based estimation of first-passage probabilities can be several orders-of-magnitude faster than direct simulation.

Discussion

Entropic barriers, which arise because of the difficulty of reaching a small number of target configurations out of a vast number of possible configurations, are in contrast to enthalpic barriers, which arise because of the difficulty of escaping local minima. The challenges of molecular dynamics result from the complicated energy landscapes associated with different biomolecular systems, and can largely be summarized by these two different kinds of barriers. Most of the existing methodology focuses on enthalpic barriers, where the central picture consists of an energy landscape with a multitude of local minima separated by high energetic barriers. A less studied picture includes entropic barriers—large flat regions of the energy landscape. Accurate simulations of dynamical systems involving large single molecules, or multitudes of molecules, will typically require a better understanding of both kinds of barrier.

Sometimes, entropic barriers can be circumvented. We have provided conditions under

which direct simulation of a diffusion across a nearly flat landscape, as in a "golf-course type potential," can be replaced by the computation of the "local capacity" in the neighborhood of each target. The approach is appropriate when the first-passage probabilities, rather than first-passage times, are the objects of interest. Specifically, we give conditions under which the first-passage probabilities are approximately invariant to the initial configuration, as long as that configuration is moderately removed from each target region. In turn, a consequence of this invariance is that the hitting probabilities can be approximated using only local computations, or simulations, around the targets. Numerical experiments on a prototypical entropic barrier, with a golf-course potential, demonstrate the validity of these results and the effectiveness of the approximations.

To what extent can these results contribute to the understanding of the folding of a large biopolymer? As a specific example, consider the folding of an RNA molecule, starting from either a denatured state or an intermediate state characterized by a non-native secondary structure. That is, some of the existing stems are not part of the native structure or additional stems will eventually appear. Assume that stem formation and destruction are sufficiently rapid to be considered as immediate events in the time-scale of folding. In the former case because stems, once seeded, are completed rapidly[28], and in the latter case because large-deviations, once they occur, occur rapidly. Given the current state, what happens next?

Put aside, for the time being, the possibility of an existing stem unfolding, and assume that there are enough internal degrees of freedom that are sufficiently unconstrained so as to constitute an entropic barrier to the search for seeding a new stem. The available stems are easy to delineate, and each one can be considered a target, defined in terms of its own reaction coordinates. As shown here, target capacities can be estimated and used to construct a distribution over the ensemble of available stems. A choice from this distribution amounts to a shortcut around the entropic barrier. The geometry is certainly complicated, with boundaries defined by physical limits on bond configurations, including allowed dihedral angles, bond separations, and so-on. But movements that are within these constraints and at the same time distant from targets will likely be largely free of substantial gradients. In such cases the analyses presented here could be useful for predicting the next stem formation. Depending on the native structure, at some point in its folding trajectory the molecule may reach a state in which the secondary structure is sufficiently rich and

constraining that the dynamics would face little if any meaningful entropic barriers. In this regime, efforts to recapitulate the pathway would necessarily rely on direct simulation or other types of approximations, e.g. one of the variants of transition-path sampling.

More generally, these considerations will apply to the extent that a folding pathway can be viewed as a discrete-state random walk, from one secondary structure to a neighboring secondary structure (cf. Zhao et al.[36]), and to the extent that each addition involves traversing large flat regions of configuration space. Obviously, there are many challenges, but perhaps chief among them is the loss of information about first-passage times. How are we to know whether a new stem will be seeded before an old stem unravels? More generally, what are the relative probabilities of transitions to neighboring states when some of these are defined by the unraveling of substructures? The answer may require a resolution, or marriage, of two approaches, one designed for enthalpic barriers, such as the barrier preventing a stem from unraveling, and the other designed for entropic barriers, such as the barrier in the way of the self intersection needed to seed a new stem. The former naturally addresses rates and time scales, but these are mostly unavailable in the approach to entropic barriers conceived here.

APPENDIX

Three Perspectives on Hitting Probabilities

Many of our results are based on the fact that hitting probabilities can actually be seen from three distinct perspectives. Let $A, B \subset \Omega$, disjoint, open with smooth boundary.

1. Hitting probabilities. Let $\tau_S \triangleq \inf\{t : X_t \in S\}$ for any set S and $h_{A,B}(x) \triangleq \mathbb{P}(X_{\tau_{A\cup B}} \in \partial A | X_0 = x)$.

2. Elliptic equation. Let $h^{\text{dir}}_{A,B}(x)$ denote the solution to the partial differential equation:

$$0 = \sum_{i=1}^{n} b_i(x)\frac{\partial u(x)}{\partial x_i} + \frac{1}{2}\sum_{i=1}^{n}\sum_{j=1}^{n} a_{ij}(x)\frac{\partial^2 u(x)}{\partial x_i \partial x_j} \quad x \notin \bar{A}, \bar{B} \tag{A1}$$

$$1 = u(x), x \in A$$

$$0 = u(x), x \in B$$

$$0 = \mathfrak{n}(x)^T a(x) \nabla u(x), x \in \partial\Omega$$

   This solution is unique and smooth.[22] What's more, it is equal to the hitting probability function: $h^{\text{dir}}_{A,B}(x) = h_{A,B}(x)$ (cf. Section 6.7 of Chen[9]).

3. Variational form. For any open set $S \subset \Omega$ let $\mathscr{E}_S(f,g) \triangleq \int_S \nabla f(x)^T a(x) \nabla g(x) \rho(dx)$ denote the "Dirichlet Form" of f, g on the domain S. Let $\mathscr{L}^2(S,\rho)$ denote the Hilbert space of functions on S which are square-integrable with respect to ρ. Let $\mathcal{H}^1(S,\rho) = W^{1,2}(S) \subset \mathscr{L}^2(S)$ denote the corresponding once-weakly-differentiable Hilbert Sobolev space. We define $h^{\text{var}}_{A,B}(x)$ as the solution to

$$\begin{aligned} \min_{u \in \mathcal{H}^1(S)} \quad & \mathscr{E}_S(u,u) \\ \text{subject to} \quad & u(x) = 1, x \in \partial A \\ & u(x) = 0, x \in \partial B \end{aligned}$$

   where $S = \Omega \backslash (A \cup B)$. This solution is unique and equal to $h^{\text{dir}}_{A,B}$ on S (cf. Section 4 of Dret[14]). This variational perspective leads us to the notion of the "condenser

capacity" associated with $h_{A,B}$. It is defined as

$$\text{cap}(A, \Omega \backslash B) \triangleq \mathscr{E}_S(h_{A,B}, h_{A,B})$$

where again $S = \Omega \backslash (A \cup B) = (\Omega \backslash B) \backslash A$.

We will use all three of these perspectives to show our results. For example, consider how the hitting probability perspective helps us show a result about capacities:

Proposition 2. *Let $A \subset \tilde{A}, B \subset \tilde{B}$ with $\tilde{A}, \tilde{B}$ disjoint. Then*

$$\text{cap}(A \cup B, \tilde{A} \cup \tilde{B}) = \text{cap}(A, \tilde{A}) + \text{cap}(B, \tilde{B})$$

Proof. Since $\tilde{A}, \tilde{B}$ are disjoint and X is continuous, the process cannot cross from one to the other without hitting the boundary. Thus we have $\tau_{\partial \tilde{A} \cup \partial \tilde{B} \cup \partial A \cup \partial B} = \tau_{\partial \tilde{A} \cup \partial A}$ as long as $X_0 \in \tilde{A}$. We get a symmetric result if $X_0 \in \tilde{B}$. It follows that

$$h_{A \cup B, (\tilde{A} \cup \tilde{B})^c}(x) = \begin{cases} h_{A, \tilde{A}^c}(x) & \text{if } x \in \tilde{A} \\ h_{B, \tilde{B}^c}(x) & \text{if } x \in \tilde{B} \end{cases}$$

We can now use this probabilistic perspective to help us understand the capacity by articulating it as the Dirichlet form on the relevant hitting probability functions

$$\begin{aligned} \text{cap}(A \cup B, \tilde{A} \cup \tilde{B}) &= \int_{\tilde{A} \cup \tilde{B} \backslash (A \cup B)} \|\sigma \nabla h_{A \cup B, (\tilde{A} \cup \tilde{B})^c}\|^2 \rho(dx) \\ &= \int_{\tilde{A} \backslash A} \|\sigma \nabla h_{A, \tilde{A}^c}\|^2 \rho(dx) + \int_{\tilde{B} \backslash B} \|\sigma \nabla h_{B, \tilde{B}^c}\|^2 \rho(dx) \\ &= \text{cap}(A, \tilde{A}) + \text{cap}(B, \tilde{B}) \end{aligned}$$

as desired. □

Proof of Theorem 2

A stationary reversible diffusion X is trapped inside the a convex open n-dimensional set with diameter 1. We are interested to know which target X will hit first: $A = \mathcal{B}(x_A, r_A)$ or

$B = \mathcal{B}(x_B, r_B)$. The function $h_{A,B}(x)$ indicates the probability we will hit A first if $X_0 = x$. We will be particularly interested in the case where X_0 is outside of $\tilde{A} = \mathcal{B}(x_A, r_{\tilde{A}}), \tilde{B} = \mathcal{B}(x_A, r_{\tilde{B}})$. Also recall that in the toy example the diffusion behaves as a Brownian motion outside of $\dot{A} = \mathcal{B}(x_A, r_{\dot{A}}), \dot{B} = \mathcal{B}(x_B, r_{\dot{B}})$.

It turns out that by taking n to be sufficiently high or $r_{\dot{A}}, r_{\dot{B}}$ to be sufficiently small, we can make the hitting probabilities arbitrarily close to constant in the region away from $\tilde{A}, \tilde{B}$. This is the content of Theorem 2 from the main text, which we restate here for the convenience of the reader:

Theorem 2. *If $\nabla U(x) = 0$ on $x \in \Omega \backslash (\tilde{A} \cup \tilde{B})$, then for any fixed value of the dimension $n \geq 3$ and any $r_{\tilde{A}}, r_{\tilde{B}}, \varepsilon > 0$, there exists a constant $c = c(n, r_{\tilde{A}}, r_{\tilde{B}}, \varepsilon)$ such that if $r_{\dot{A}}, r_{\dot{B}} < c$ then $h_{A,B}(x)$ is ε-flat relative to $\Omega/(\tilde{A} \cup \tilde{B})$. Likewise, for any fixed values of $r_{\dot{A}}, r_{\tilde{A}}, r_{\dot{B}}, r_{\tilde{B}}, \varepsilon > 0$, there exists a constant $c = c(r_{\dot{A}}, r_{\tilde{A}}, r_{\dot{B}}, r_{\tilde{B}}, \varepsilon)$ such that if $n \geq c$ then $h_{A,B}(x)$ is ε-flat relative to $\Omega/(\tilde{A} \cup \tilde{B})$.*

Proof. Let us assume $X_0 \notin \tilde{A}, \tilde{B}$. There are essentially two things that must be proved:

1. The process X converges to its stationary distribution fairly quickly. This is supported by Lemma 1. Since $h_{A,B}(x) \in [0, 1]$, this Lemma gives that

$$|\mathbb{E}[h_{A,B}(M_t) - h_{A,B}(Z)]| \leq 2^2/4t = 1/t$$

   where Z is distributed according to the uniform distribution on Ω and M is a Brownian motion trapped in Ω by normally reflecting boundaries.

   To connect this result on M to our object of interest $h_{A,B}$, note that without loss of generality we may assume X, M are on the same probability space and $M_t = X_t$ for $t < \tilde{\tau} \triangleq \inf\{t : \ X_t \in \partial\dot{A} \cup \partial\dot{B}\}$. Moreover, note that $\forall t \geq 0$, $\tilde{\tau} \wedge t$ is a stopping time with finite expectation, and $h_{A,B}$ is a solution to the elliptic equation A1. Applying Dynkin's formula, we observe that

$$h_{A,B}(x) = \mathbb{E}[h_{A,B}(X_{t \wedge \tilde{\tau}})] = \mathbb{E}[h_{A,B}(M_{t \wedge \tilde{\tau}})]$$

Thus

$$\begin{aligned}|h_{A,B}(x) - \mathbb{E}[h_{A,B}(Z)]| &= |\mathbb{E}[h_{A,B}(M_{t\wedge\tilde{\tau}})] - \mathbb{E}[h_{A,B}(Z)]| \\ &\leq |\mathbb{E}[h_{A,B}(M_{t\wedge\tilde{\tau}})] - h_{A,B}(M_t)]| + |\mathbb{E}[h_{A,B}(M_t) - h_{A,B}(Z)]| \\ &\leq \mathbb{P}(\tilde{\tau} \leq t) + 1/t\end{aligned}$$

2. The hitting time $\tilde{\tau}$ is generally long. This is supported by Lemma 2, which says that if $X_0 \notin \tilde{A} \cup \tilde{B}$ we can ensure

$$\mathbb{P}\left(\tilde{\tau} \leq t\right) < \varepsilon/2$$

for arbitrarily small ε and arbitrarily large t, by taking n sufficiently high or $r_{\dot{A}}, r_{\dot{B}}$ sufficiently small.

Putting these two results together at $t = 2/\varepsilon$ we obtain that we can make $|h_{A,B}(x) - \mathbb{E}[h_{A,B}(Z)]| \leq \varepsilon/2 + \varepsilon/2 = \varepsilon$ for arbitrarily small ε by taking n sufficiently high or $r_{\dot{A}}, r_{\dot{B}}$ sufficiently small. □

Lemma 1. *(Uniform ergodicity) Let $\Omega \subset \mathbb{R}^d$ be a convex set with diameter ξ and let M denote a Brownian motion trapped by reflecting boundaries inside Ω. The distribution of M_t converges uniformly to the uniform distribution, in the sense that:*

$$\sup_{f:\ \Omega\to[0,1]} |\mathbb{E}[f(M_t) - f(Z)|M_0 = x]| \leq \xi^2/4t \qquad \forall x \in \Omega, t > 0$$

where Z is uniformly distributed on Ω.

Proof. Per Loper [24],

$$\sup_{f:\ \Omega\to[0,1]} |\mathbb{E}[f(M_t) - f(Z)|M_0 = x]| \leq \mathbb{P}(\tau > 4t)$$

where τ is the first exit time of a one-dimensional Brownian motion from the interval $[-\xi, \xi]$ when initialized at the origin. Dynkin's formula gives that $\mathbb{E}[\tau] = \xi^2$. Hence, by the Markov inequality, $\mathbb{P}(\tau > 4t) \leq \xi^2/4t$. □

Lemma 2. *Let $\tilde{\tau} = \inf\{t : X_t \in \dot{A} \cup \dot{B}\}$. For any fixed value of $n \geqslant 3$ and $r_{\tilde{A}}, r_{\tilde{B}}, \varepsilon, t > 0$,*

there exists some $c(n, r_{\tilde{A}}, r_{\tilde{B}}, \varepsilon, t)$ *such that if* $r_{\dot{A}}, r_{\dot{B}} < c$*, then*

$$\mathbb{P}\left(\tilde{\tau} < t | X_0 \notin \tilde{A} \cup \tilde{B}\right) < \varepsilon$$

Likewise, for any fixed value of $r_{\dot{A}}, r_{\tilde{A}}, r_{\dot{B}}, r_{\tilde{B}}, \varepsilon, t > 0$*, there exists some* $c(r_{\dot{A}}, r_{\tilde{A}}, r_{\dot{B}}, r_{\tilde{B}}, \varepsilon, t)$*, such that the same property holds as long as* $n \geqslant c$*.*

Proof. Our task is to show that $\tilde{\tau}$ is large with high probability. Note that it suffices to show that $\tilde{\tau}_A \triangleq \inf\{t : \ X_t \in \dot{A}\}$ and $\tilde{\tau}_B \triangleq \inf\{t : \ X_t \in \dot{B}\}$ are both large with high probability and then apply a union bound. Thus, without loss of generality we will focus on showing that $\tilde{\tau}_A$ is large with high probability. For this, Chernoff's bound shows that it would be sufficient to show that we can make

$$g(x) = \mathbb{E}[e^{-\frac{1}{2}\tilde{\tau}_A} | X_0 = x]$$

arbitrarily small for every $x \notin \tilde{A}$. We note that $\forall X_0 \notin \tilde{A}$, the continuity of X dictates that X would have to cross the set $S_{\tilde{r}_{\dot{A}}} = \{x : \ |x - x_A| = \tilde{r}_{\dot{A}}\}$ before $\tilde{\tau}_A$, as long as $\tilde{r}_{\dot{A}} \in (r_{\dot{A}}, r_{\tilde{A}})$. Applying the strong Markov property of X, we obtain $g(x) \leq \sup_{y \in S_{\tilde{r}_{\dot{A}}}} g(y), \forall x \notin \tilde{A}$. As a result, to prove our theorem it will suffice to show that by taking $r_{\dot{A}}$ sufficiently small or n sufficiently large we can ensure that $g(x)$ is uniformly arbitrarily small on $S_{\tilde{r}_{\dot{A}}}$ for some $\tilde{r}_{\dot{A}} \in (r_{\dot{A}}, r_{\tilde{A}})$. To show this, we will make use of two other hitting times:

$$T = \inf\{t : \ X_t \notin \tilde{A} \backslash \dot{A}\} \qquad T_1 = \inf\{t \geq T : \ X_t \in S_{\tilde{r}_{\dot{A}}}\}$$

$\forall X_0 \in S_{\tilde{r}_{\dot{A}}}$, if $X_T \notin \partial\dot{A}$, then the process exits $\tilde{A} \backslash \dot{A}$ at $\partial\tilde{A}$, and would have to cross $S_{\tilde{r}_{\dot{A}}}$ again before reaching $\dot{A}$. In this case, we have $T_1 \leq \tilde{\tau}_A$. Applying the strong Markov property, we see that $\forall x \in S_{\tilde{r}_{\dot{A}}}$

$$\begin{aligned}
g(x) =& \mathbb{E}[e^{-\frac{1}{2}\tilde{\tau}_A} \mathbb{I}_{X_T \in \partial\dot{A}} | X_0 = x] + \mathbb{E}[e^{-\frac{1}{2}\tilde{\tau}_A} \mathbb{I}_{X_T \in \partial\tilde{A}} | X_0 = x] \\
=& \mathbb{E}[e^{-\frac{1}{2}\tilde{\tau}_A} \mathbb{I}_{T = \tilde{\tau}_A} | X_0 = x] + \mathbb{E}[e^{-\frac{1}{2}\tilde{\tau}_A} \mathbb{I}_{T \neq \tilde{\tau}_A} | X_0 = x] \\
=& \mathbb{E}[e^{-\frac{1}{2}\tilde{\tau}_A} \mathbb{I}_{T = \tilde{\tau}_A} | X_0 = x] + \mathbb{E}[e^{-\frac{1}{2}T_1} g(X_{T_1}) \mathbb{I}_{T \neq \tilde{\tau}_A} | X_0 = x] \\
\leq& \mathbb{E}[e^{-\frac{1}{2}T} \mathbb{I}_{T = \tilde{\tau}_A} | X_0 = x] + \mathbb{E}[e^{-\frac{1}{2}T} \mathbb{I}_{T \neq \tilde{\tau}_A} | X_0 = x] \left(\sup_{y \in S_{\tilde{r}_{\dot{A}}}} g(y) \right)
\end{aligned}$$

Note furthermore that the law of $e^{-\frac{1}{2}T}, \mathbb{I}_{T=\tilde{\tau}_A}$ is actually the same for every $x \in S_{\tilde{r}_{\dot{A}}}$, due to the fact that the diffusion behaves simply like a Brownian motion inside $\tilde{A}\backslash\dot{A}$ and the law of $T, \mathbb{I}_{T=\tau_A}$ are thus functions of the one-dimensional diffusion of $|X_t - x_A|$. In fact, Wendel[33] gives explicit formulas for $\mathbb{E}[e^{-\frac{1}{2}T}\mathbb{I}_{T=\tilde{\tau}_A}|X_0 = x], \mathbb{E}[e^{-\frac{1}{2}T}\mathbb{I}_{T\neq\tilde{\tau}_A}|X_0 = x]$ which depend only upon $|x - x_A|, r_{\tilde{A}}, r_{\dot{A}}$. Applying this, taking the supremum over x of our previous formula, and rearranging, we obtain

$$\sup_{x\in S_{\tilde{r}_{\dot{A}}}} g(x) \leq \frac{\mathbb{E}[e^{-\frac{1}{2}T}\mathbb{I}_{T=\tilde{\tau}_A}|X_0 \in S_{\tilde{r}_{\dot{A}}}]}{1 - \mathbb{E}[e^{-\frac{1}{2}T}\mathbb{I}_{T\neq\tilde{\tau}_A}|X_0 \in S_{\tilde{r}_{\dot{A}}}]} \triangleq L(r_{\dot{A}}, \tilde{r}_{\dot{A}}, r_{\tilde{A}}, n)$$

Applying Wendel's formulas, we obtain a closed form expression for L:

$$= \frac{\left(\frac{r_{\dot{A}}}{\tilde{r}_{\dot{A}}}\right)^h (I_h(r_{\tilde{A}})K_h(\tilde{r}_{\dot{A}}) - I_h(\tilde{r}_{\dot{A}})K_h(r_{\tilde{A}}))}{\left(\frac{I_h(r_{\tilde{A}})}{I_h(\tilde{r}_{\dot{A}})} - \left(\frac{r_{\tilde{A}}}{\tilde{r}_{\dot{A}}}\right)^h\right) K_h(r_{\dot{A}})I_h(\tilde{r}_{\dot{A}}) + \left(\left(\frac{r_{\tilde{A}}}{\tilde{r}_{\dot{A}}}\right)^h - \frac{K_h(r_{\tilde{A}})}{K_h(\tilde{r}_{\dot{A}})}\right) I_h(r_{\dot{A}})K_h(\tilde{r}_{\dot{A}})}$$

where $h = (n-2)/2$ and I_h, K_h represent modified Bessel functions of the first and second kind of order h.

Thus, to complete our proof, it suffices to show that we can drive $L(r_{\dot{A}}, \tilde{r}_{\dot{A}}, r_{\tilde{A}}, n)$ to zero by taking $r_{\dot{A}}$ small or n large:

- When $r_{\dot{A}}$ is small. The numerator of L converges to zero as $r_{\dot{A}} \to 0$, because $\frac{r_{\dot{A}}}{\tilde{r}_{\dot{A}}} \to 0, h > 0$ and the other terms are constant. On the other hand, the denominator explodes, because as $r_{\dot{A}} \to 0$ we have

$$\left(\frac{I_h(r_{\tilde{A}})}{I_h(\tilde{r}_{\dot{A}})} - \left(\frac{r_{\tilde{A}}}{\tilde{r}_{\dot{A}}}\right)^h\right) K_h(r_{\dot{A}})I_h(\tilde{r}_{\dot{A}}) \to +\infty$$
$$\left(\left(\frac{r_{\tilde{A}}}{\tilde{r}_{\dot{A}}}\right)^h - \frac{K_h(r_{\tilde{A}})}{K_h(\tilde{r}_{\dot{A}})}\right) I_h(r_{\dot{A}})K_h(\tilde{r}_{\dot{A}}) \to 0$$

  These limits follow immediately from three properties of Bessel functions:

  - $K_h(x) \to \infty, I_h(x) \to 0$ as $x \to 0$ for $h > 0$
  - $K_h(x), I_h(x) > 0$ for $x > 0, h > 0$
  - $\frac{I_h(y)}{I_h(x)} > \left(\frac{y}{x}\right)^h$ for $y > x$ and $h > 0$

The first two properties are well-known and can be found in DLMF[1]; the second can be found in Baricz.[1, 3] In conclusion, since the numerator vanishes and the denominator explodes, we have that overall L vanishes.

- When n is large. It is clear that the previous result holds for any value of $\tilde{r}_{\dot{A}} \in (r_{\dot{A}}, r_{\tilde{A}})$. For the large-$n$ case, we will be more picky: we will take $\tilde{r}_{\dot{A}} = \sqrt{r_{\dot{A}} r_{\tilde{A}}}$.

  Let us look at the numerator first. Asymptotics from the DLMF give that as $h = (n-2)/2 \to \infty$ we have

$$I_h(x) \sim \frac{x^h}{2^h \Gamma(h+1)} \qquad\qquad K_h(x) \sim \frac{2^h \Gamma(h+1)}{(2h) x^h}$$

  Here by $f_1(h) \sim f_2(h)$ we mean "asymptotic equivalence," i.e. $\lim_{h\to\infty} f_1(h)/f_2(h) = 1$. Applying to our case:

$$\left(\frac{r_{\dot{A}}}{\tilde{r}_{\dot{A}}}\right)^h I_h(r_{\tilde{A}}) K_h(\tilde{r}_{\dot{A}}) \sim \frac{1}{2h} \left(\frac{r_{\tilde{A}} r_{\dot{A}}}{\tilde{r}_{\dot{A}}^2}\right)^h = \frac{1}{2h} \to 0$$
$$\left(\frac{r_{\dot{A}}}{\tilde{r}_{\dot{A}}}\right)^h I_h(\tilde{r}_{\dot{A}}) K_h(r_{\tilde{A}}) \sim \frac{1}{2h} \left(\frac{r_{\dot{A}}}{r_{\tilde{A}}}\right)^h \to 0$$

  Putting these two limits together we see that the numerator of L is asymptotically vanishing.

  Now let us turn to the denominator. First note that

$$\left(\frac{r_{\tilde{A}}}{\tilde{r}_{\dot{A}}}\right)^h I_h(r_{\dot{A}}) K_h(\tilde{r}_{\dot{A}}) \sim \frac{1}{2h} \left(\frac{r_{\tilde{A}} r_{\dot{A}}}{\tilde{r}_{\dot{A}}^2}\right)^h = \frac{1}{2h} \to 0$$
$$-\frac{K_h(r_{\tilde{A}})}{K_h(\tilde{r}_{\dot{A}})} I_h(r_{\dot{A}}) K_h(\tilde{r}_{\dot{A}}) \sim -\frac{1}{2h} \left(\frac{r_{\dot{A}}}{r_{\tilde{A}}}\right)^h \to 0$$

  So those terms are negligible. However, the other two terms of the denominator are in fact exploding: one to positive infinity and one to negative infinity. To understand this delicate balance, we these we turn to Lemma 3. Applying this Lemma and the

asymptotics of the DLMF, we obtain that

$$\begin{aligned}\left(\frac{I_h(r_{\tilde{A}})}{I_h(\tilde{r}_{\dot{A}})} - \left(\frac{r_{\tilde{A}}}{\tilde{r}_{\dot{A}}}\right)^h\right) K_h(r_{\dot{A}})I_h(\tilde{r}_{\dot{A}}) &\geq \frac{r_{\tilde{A}}^h}{\cancel{I_h(\tilde{r}_{\dot{A}})}} \times \frac{r_{\tilde{A}}^2 - \tilde{r}_{\dot{A}}^2}{2^{h+2}\Gamma(h+2)} K_h(r_{\dot{A}})\cancel{I_h(\tilde{r}_{\dot{A}})} \\ &\sim r_{\tilde{A}}^h \times \frac{r_{\tilde{A}}^2 - \tilde{r}_{\dot{A}}^2}{2^{h+2}\Gamma(h+2)} \frac{2^h\Gamma(h+1)}{2hr_{\dot{A}}^h} \\ &= \left(\frac{r_{\tilde{A}}}{r_{\dot{A}}}\right)^h \left(\frac{r_{\tilde{A}}^2 - \tilde{r}_{\dot{A}}^2}{8h(h+1)}\right)\end{aligned}$$

which is indeed exploding as $h = (n-2)/2 \to \infty$.

In conclusion, with this choice of $\tilde{r}_{\dot{A}}$, the numerator is asymptotically vanishing, but the denominator is asymptotically exploding. Thus L vanishes.

Let us now review our arguments to see how the vanishing of L leads to our desired conclusion. We have just shown that by taking n large or $r_{\dot{A}}$ small, we can ensure that L vanishes. Thus for any $x_0 \notin \tilde{A}$ and any $\varepsilon' > 0$, we can ensure

$$\begin{aligned}\varepsilon' \geq L &\geq \sup_{y \in S_{\tilde{r}_{\dot{A}}}} g(y) \geq g(x) \\ &= \mathbb{E}[e^{-\frac{1}{2}\tilde{\tau}_A} | X_0 = x] \\ &\geq \mathbb{P}(\tilde{\tau}_A < t) e^{\frac{1}{2}t}\end{aligned}$$

In particular, for any $t, \varepsilon > 0$ we can ensure that $\mathbb{P}(\tilde{\tau}_A < t) < \varepsilon/2$ by ensuring $\varepsilon' < \varepsilon e^{-\frac{1}{2}t}/2$. We can then ensure that $\mathbb{P}(\tilde{\tau} < t) < \varepsilon$ by applying the same arguments to $\tilde{\tau}_B$ and applying a union bound.

□

Lemma 3. *If $a > b$ then*

$$\frac{I_h(a)}{I_h(b)} - \left(\frac{a}{b}\right)^h \geq \frac{a^h}{I_h(b)} \times \frac{a^2 - b^2}{2^{h+2}\Gamma(h+2)}$$

Proof. Recall that I_h may be defined as

$$I_h(x) = \sum_{m=0}^{\infty} \frac{x^{h+2m}}{2^{h+2m}\Gamma(m+h+1)\Gamma(m+1)}$$

Thus

$$\frac{I_h(a)}{I_h(b)} - \left(\frac{a}{b}\right)^h = \frac{I_h(a)b^h - a^h I_h(b)}{b^h I_h(b)} = \frac{a^h b^h \sum_{m=0}^{\infty} \frac{a^{2m}-b^{2m}}{2^{h+2m}\Gamma(m+h+1)\Gamma(m+1)}}{b^h I_h(b)}$$

Since $a > b$, we have that $a^{2m} - b^{2m}$ is always positive. Thus we can get a lower bound by simply taking one of the terms. Choosing $m = 1$, we get our final result. □

Proof of Theorem 1

Let $A \subset \tilde{A} \subset \Omega, B \subset \tilde{B} \subset \Omega$. Let $\tilde{A}, \tilde{B}$ be disjoint and $h_{A,B}(x)$ ε-flat with respect to $\Omega \backslash (\tilde{A} \cup \tilde{B})$. We assume the set boundaries are all smooth.

Under these conditions, we will show we can use local capacities to get good approximations for $h_{A,B}(x)$ when $x \notin \tilde{A}, \tilde{B}$. To do so, our key idea is to uncover upper and lower bounds on the value of the Dirichlet form applied to this function, $\mathscr{E}(h_{A,B}, h_{A,B})$. We will see that these bounds can be understood in terms of local capacities, and the resulting inequalities will then yield our main result in the form of Theorem 1.

Lemma 4. *Let $S = \Omega \backslash (A \cup B)$. The Dirichlet form of $h_{A,B}$ on S can be upper-bounded in terms of the capacities:*

$$\mathscr{E}_S(h_{A,B}, h_{A,B}) \leqslant \frac{\operatorname{cap}(A, \tilde{A}) \operatorname{cap}(B, \tilde{B})}{\operatorname{cap}(A, \tilde{A}) + \operatorname{cap}(B, \tilde{B})}$$

Proof. We recall from Appendix A that

$$\mathscr{E}_S(h_{A,B}, h_{A,B}) = \operatorname{cap}(A, \Omega \backslash B) \leq \mathscr{E}_S(u, u)$$

for any u with $u(\partial A) = 1, u(\partial B) = 0$. Thus, to prove an upper bound it suffices to find any

such function for which we can calculate $\mathscr{E}(u,u)$. To this end, consider

$$u_c(x) \triangleq \begin{cases} (1-c)h_{A,\tilde{A}^c}(x) + c & \text{if } x \in \tilde{A} \\ c(1-h_{B,\tilde{B}^c}(x)) & \text{if } x \in \tilde{B} \\ c & \text{otherwise} \end{cases}$$

These functions are well-suited to giving us upper bounds on $\mathscr{E}_S(h_{A,B}, h_{A,B})$. Indeed:

- $u_c(\partial A) = 1, u_c(\partial B) = 0$. In fact, u_c takes a constant value c outside of $\tilde{A}, \tilde{B}$, drops smoothly in $\tilde{B}$ to achieve 0 on ∂B, and rises smoothly in $\tilde{A}$ to achieve 1 on $\partial \tilde{A}$.
- Noting that u_c is written as a piecewise combination of hitting probability functions, we see that its Dirichlet form can be calculated in terms of capacities on local regions: $\mathscr{E}_S(u_c, u_c) = (1-c)^2 \operatorname{cap}(A, \tilde{A}) + c^2 \operatorname{cap}(B, \tilde{B})$.

Thus the u_c functions give us a practical way to calculate upper bounds:

$$\mathscr{E}_S(h_{A,B}, h_{A,B}) \leq (1-c)^2 \operatorname{cap}(A, \tilde{A}) + c^2 \operatorname{cap}(B, \tilde{B})$$

This inequality holds for any value of c. To get the best bound, we can take derivatives to minimize the right hand side with respect to c. The result is

$$c^* = \frac{\operatorname{cap}(A, \tilde{A})}{\operatorname{cap}(A, \tilde{A}) + \operatorname{cap}(B, \tilde{B})}$$

Plugging this into the previous equation, we obtain our final result. □

Lemma 5. *Let $S = \Omega \backslash (A \cup B)$. Let $m = \frac{1}{2}(\sup_{x \notin \tilde{A}, \tilde{B}} h_{A,B}(x) + \inf_{x \notin \tilde{A}, \tilde{B}} (h_{A,B}(x)))$. The Dirichlet form of $h_{A,B}$ can be lower-bounded in terms of m and the capacities:*

$$\mathscr{E}_S(h_{A,B}, h_{A,B}) \geq \left(1 - m - \frac{\varepsilon}{2}\right)^2 \operatorname{cap}(A, \tilde{A}) \mathbb{I}_{m \leq 1 - \frac{\varepsilon}{2}} + \left(m - \frac{\varepsilon}{2}\right)^2 \operatorname{cap}(B, \tilde{B}) \mathbb{I}_{m \geq \frac{\varepsilon}{2}}$$

Proof. Recall that $\mathscr{E}_S(h_{A,B}, h_{A,B})$ can be expressed as an integral over S. We decompose this into three integrals: one over $\tilde{A}$, one over $\Omega \backslash \tilde{A}, \tilde{B}$, and one over $\tilde{B}$.

$$\mathscr{E}_S(h_{A,B}, h_{A,B}) = \int_{\tilde{A} \backslash A} \|\sigma \nabla h_{A,B}\|^2 \rho(dx) + \int_{\tilde{B} \backslash B} \|\sigma \nabla h_{A,B}\|^2 \rho(dx) + \int_{\Omega \backslash \tilde{A}, \tilde{B}} \|\sigma \nabla h_{A,B}\|^2 \rho(dx)$$

Since the integrand is always positive, we can get a lower bound by simply ignoring the integral over $\Omega\backslash\tilde{A},\tilde{B}$ and focusing on the integrals over $\tilde{A},\tilde{B}$. The $\tilde{A},\tilde{B}$ integrals can be lower-bounded using capacities.

For example, let us focus on the A integral. There are two different possibilities we must consider:

- If $m > 1-\varepsilon/2$ we will simply note that the integral over the $\tilde{A}$ region is non-negative.

- If $m \leq 1-\varepsilon/2$, then we define

$$u_A(x) \triangleq \frac{h_{A,B}(x) - m - \frac{\varepsilon}{2}}{1 - m - \frac{\varepsilon}{2}}$$

  Note that $h_{A,B}(x) = 1$ for $x \in \partial A$ and the ε-flatness condition shows that $h_{A,B}(x) \leq m + \frac{\varepsilon}{2}$ for $x \in \partial\tilde{A}$. Thus $u_A(\partial A) \geq 1, u_A(\partial\tilde{A}) \leq 0$. Lemma 7 from Appendix E may then be applied to yield that $\mathscr{E}_{\tilde{A}\backslash A}(u_A,u_A) \geq \mathrm{cap}(A,\tilde{A})$. We can thus obtain the bound

$$\begin{aligned}\int_{\tilde{A}\backslash A} \|\sigma\nabla h_{A,B}\|^2\rho(dx) &= \left(1-m-\frac{\varepsilon}{2}\right)^2 \mathscr{E}_{\tilde{A}\backslash A}(u_A,u_A)\\ &\geq \left(1-m-\frac{\varepsilon}{2}\right)^2 \mathrm{cap}(A,\tilde{A})\end{aligned}$$

Putting these two possibilities together, we obtain

$$\int_{\tilde{A}\backslash A} \|\sigma\nabla h_{A,B}\|^2\rho(dx) \geq \left(1-m-\frac{\varepsilon}{2}\right)^2 \mathrm{cap}(A,\tilde{A})\mathbb{I}_{m\leq 1-\frac{\varepsilon}{2}}$$

Applying the same ideas to the integral over $\tilde{B}$, we obtain our result. □

We are now in a position to prove Theorem 1 from the main text:

Theorem 1. *Assume that $h_{A,B}(x)$ is ε-flat relative to $\Omega\backslash(\tilde{A}\cup\tilde{B})$. Then the first-passage probabilities can be well-approximated in terms of the target capacities:*

$$\sup_{x\notin\tilde{A},\tilde{B}} \left| h_{A,B}(x) - \frac{\mathrm{cap}(A,\tilde{A})}{\mathrm{cap}(A,\tilde{A}) + \mathrm{cap}(B,\tilde{B})} \right| \leqslant \varepsilon + \sqrt{\varepsilon/2}$$

Proof. To simplify notation, let $\kappa_A = \mathrm{cap}(A, \tilde{A})$ and $\kappa_B = \mathrm{cap}(B, \tilde{B})$. Applying the previous two lemmas together, we obtain the inequality

$$\frac{\kappa_A \kappa_B}{\kappa_A + \kappa_B} \geq \mathscr{E}(h_{A,B}, h_{A,B}) \geq \left(1 - m - \frac{\varepsilon}{2}\right)^2 \kappa_A \mathbb{I}_{m \leq 1 - \frac{\varepsilon}{2}} + \left(m - \frac{\varepsilon}{2}\right)^2 \kappa_B \mathbb{I}_{m \geq \frac{\varepsilon}{2}}$$

where $m = \frac{1}{2}(\sup_{x \notin \tilde{A}, \tilde{B}} h_{A,B}(x) + \inf_{x \notin \tilde{A}, \tilde{B}}(h_{A,B}(x)))$. In analyzing this inequality, there are three possibilities to consider.

- If $m \in (\varepsilon/2, 1 - \varepsilon/2)$, the quadratic formula yields

$$m \geqslant \frac{\kappa_A}{\kappa_A + \kappa_B} + \frac{\frac{\varepsilon}{2}(\kappa_B - \kappa_A) - \sqrt{\kappa_A \kappa_B \varepsilon(2 - \varepsilon)}}{\kappa_A + \kappa_B}$$
$$m \leqslant \frac{\kappa_A}{\kappa_A + \kappa_B} + \frac{\frac{\varepsilon}{2}(\kappa_B - \kappa_A) + \sqrt{\kappa_A \kappa_B \varepsilon(2 - \varepsilon)}}{\kappa_A + \kappa_B}$$

  Applying $\left|\frac{\kappa_B - \kappa_A}{\kappa_A + \kappa_B}\right| \leq 1$ and the fact that the geometric mean $\sqrt{\kappa_A \kappa_B}$ never exceeds the arithmetic mean $(\kappa_A + \kappa_B)/2$, it follows that

$$\left| m - \frac{\kappa_A}{\kappa_A + \kappa_B} \right| \leq \frac{\varepsilon + \sqrt{\varepsilon(2 - \varepsilon)}}{2}$$

  Applying the fact that m was designed so that $|h_{A,B}(x) - m| < \varepsilon/2$ for all $x \notin \tilde{A}, \tilde{B}$, we obtain

$$\left| h_{A,B}(x) - \frac{\kappa_A}{\kappa_A + \kappa_B} \right| \leq \frac{2\varepsilon + \sqrt{\varepsilon(2 - \varepsilon)}}{2}$$

- If $m < \varepsilon/2$, our equations become

$$\frac{\cancel{\kappa_A}\kappa_B}{\kappa_A + \kappa_B} \geq \left(1 - m - \frac{\varepsilon}{2}\right)^2 \cancel{\kappa_A}$$

  Our assumption that $m \leq \varepsilon/2$ indicates that $(1 - m - \varepsilon/2)^2 \geq (1 - \varepsilon)^2$, thus in fact we have

$$\frac{\kappa_B}{\kappa_A + \kappa_B} \geq (1 - \varepsilon)^2 = 1 + \varepsilon^2 - 2\varepsilon$$

  which means that $\kappa_A/(\kappa_A + \kappa_B) \leq 2\varepsilon - \varepsilon^2 \leq 2\varepsilon$. Thus we assumed $m \in [0, \varepsilon/2]$ and

showed that $\kappa_A/(\kappa_A+\kappa_B) \in [0, 2\varepsilon-\varepsilon^2]$, so it follows that

$$\left| m - \frac{\kappa_A}{\kappa_A+\kappa_B} \right| \leq 2\varepsilon - \varepsilon^2$$

and so for any $x \notin \tilde{A}, \tilde{B}$, we have

$$\left| h_{A,B}(x) - \frac{\kappa_A}{\kappa_A+\kappa_B} \right| \leq 2.5\varepsilon - \varepsilon^2$$

- If $m > 1-\varepsilon/2$, the same bound can be achieved by arguments which are symmetric to those employed in $m < \varepsilon/2$:

$$\left| h_{A,B}(x) - \frac{\kappa_A}{\kappa_A+\kappa_B} \right| \leq 2.5\varepsilon - \varepsilon^2$$

Our final result is found by noting that all these bounds are upper-bounded by $\varepsilon+\sqrt{\varepsilon/2}$. □

Proof of Proposition 1

We first establish a lemma, using Green's first identity and some properties of the stationary SDE (1), under the reversibility conditions (3), relative to U:

Lemma 6. *Fix some $S \subset \Omega$ with smooth boundary. Then for any smooth function g that satisfies $\mathcal{L}g = 0$ and smooth function f,*

$$\int_S \nabla f(x)^T a(x) \nabla g(x) e^{-U(x)} dx = \int_{\partial S} f(x) \mathfrak{n}(x)^T a(x) \nabla g(x) e^{-U(x)} \mathscr{H}(dx)$$

where $\mathfrak{n}$ are the normal vectors facing out of the set S and $\mathscr{H}(dx)$ is the integral with respect to the $(n-1)$-dimensional Hausdorff measure and

$$(\mathcal{L}f)(x) \triangleq \sum_i b_i(x) \frac{\partial f(x)}{\partial x_i} + \frac{1}{2} \sum_{ij} a_{ij}(x) \frac{\partial^2 f(x)}{\partial x_i \partial x_j}$$

Proof. First, we apply Green's first identity to get

$$\begin{aligned}&\int_S \nabla f^T a \nabla g e^{-U} dx \\ &= \int_{\partial S} f \mathfrak{n}^T a \nabla g e^{-U} \mathscr{H}(dx) - \int_S f \nabla \cdot (a \nabla g e^{-U}) dx\end{aligned}$$

where

$$\nabla \cdot (a \nabla g e^{-U}) = \sum_i \frac{\partial}{\partial x_i} \left[\sum_j e^{-U} a_{ij} \frac{\partial g}{\partial x_j} \right]$$

Next, using the reversibility constraint on b from Equation (3), it's not hard to verify that

$$\nabla \cdot (a \nabla g e^{-U}) = 2 e^{-U} \mathcal{L} g = 0$$

This gives us the desired result. □

Proposition 1. *For any regions G and $\tilde{G}$ having smooth boundaries and such that $A \subset G \subset \tilde{G} \subset \tilde{A}$, $\text{cap}(A, \tilde{A},)$ can be expressed as a flux leaving $\tilde{G} \backslash G$:*

$$\text{cap}(A, \tilde{A}) = \int_{\partial(\tilde{G} \backslash G)} h_{A, \tilde{A}^c}(x) \mathfrak{n}(x)^T a(x) \nabla h_{G, \tilde{G}^c}(x) e^{-U(x)} \mathscr{H}(dx)$$

where $a(x) = \sigma(x)\sigma(x)^T$ is the diffusion matrix, $\mathscr{H}(dx)$ is the $(n-1)$-dimensional Hausdorff measure, and $\mathfrak{n}$ represents the outward-facing (relative to $\tilde{G} \backslash G$) normal vector on $\partial(\tilde{G} \backslash G)$.

Proof. First recall that $\mathcal{L} h_{A, \tilde{A}^c} = 0$ and

$$\text{cap}(A, \tilde{A}) = \int_{\tilde{A} \backslash A} \nabla h_{A, \tilde{A}^c}(x)^T a(x) \nabla h_{A, \tilde{A}^c}(x) e^{-U(x)} dx$$

Together with Lemma 6, this yields that

$$\text{cap}(A, \tilde{A}) = \int_{\partial(\tilde{A} \backslash A)} h_{A, \tilde{A}^c} \mathfrak{n}^T a \nabla h_{A, \tilde{A}^c} e^{-U} \mathscr{H}(dx) = - \int_{\partial A} \mathfrak{n}^T a \nabla h_{A, \tilde{A}^c} e^{-U} \mathscr{H}(dx) \qquad \text{(D1)}$$

where in the last step we used $h_{A, \tilde{A}^c}(x) = 1, x \in \partial A, h_{A, \tilde{A}^c}(x) = 0, x \in \partial \tilde{A}$. Also, note that the normal vector on the right hand side is pointing *out of* the set A, as is our convention. Hence then negative sign.

Next we apply Lemma 6 again to get

$$0 = \int_{G\setminus A} \cancel{\nabla(1)} a\nabla h^T_{A,\tilde{A}^c} e^{-U} dx = \int_{\partial(G\setminus A)} \mathfrak{n}^T a\nabla h_{A,\tilde{A}^c} e^{-U} \mathscr{H}(dx)$$

Combining this with Equation D1 gives us

$$\mathrm{cap}(A,\tilde{A}) = -\int_{\partial A} \mathfrak{n}^T a\nabla h_{A,\tilde{A}^c} e^{-U} \mathscr{H}(dx) = \int_{\partial G} \mathfrak{n}^T a\nabla h_{A,\tilde{A}^c} e^{-U} \mathscr{H}(dx) \tag{D2}$$

Using the facts that $h_{G,\tilde{G}^c}(x) = 1, x \in \partial G, h_{G,\tilde{G}^c}(x) = 0, x \in \partial\tilde{G}$, and $\mathcal{L}h_{G,\tilde{G}^c} = 0$, we apply Lemma 6 two more times to obtain

$$\begin{aligned}
\mathrm{cap}(A,\tilde{A}) &= \int_{\partial G} \mathfrak{n}^T a\nabla h_{A,\tilde{A}^c} e^{-U} \mathscr{H}(dx) = \int_{\partial G} h_{G,\tilde{G}^c} \mathfrak{n}^T a\nabla h_{A,\tilde{A}^c} e^{-U} \mathscr{H}(dx) \\
&= \int_{\partial(\tilde{G}\setminus G)} h_{G,\tilde{G}^c} \mathfrak{n}^T a\nabla h_{A,\tilde{A}^c} e^{-U} \mathscr{H}(dx) = \int_{\tilde{G}\setminus G} \nabla h_{G,\tilde{G}^c} a\nabla h_{A,\tilde{A}^c} e^{-U} dx \\
&= \int_{\partial(\tilde{G}\setminus G)} h_{A,\tilde{A}^c} \mathfrak{n}^T a\nabla h_{G,\tilde{G}^c} e^{-U} \mathscr{H}(dx)
\end{aligned}$$

□

Corollary. *For any region S having smooth boundary ∂S, and such that $A \subset S \subset \tilde{A}$,* $\mathrm{cap}(A,\tilde{A},)$ *can be expressed as a flux leaving S:*

$$\mathrm{cap}(A,\tilde{A}) = \int_{\partial S} \mathfrak{n}(x)^T a(x)\nabla h_{A,\tilde{A}^c}(x) e^{-U(x)} \mathscr{H}(dx)$$

where a and $\mathscr{H}(dx)$ are as defined in the Proposition, and $\mathfrak{n}$ is the outward-facing normal on ∂S.

Proof. Put $G = S$ in Equation (D2). □

Inequality Boundary Conditions for the Variational Form

Recall that $h_{A,B}(x)$ may be defined variationally. We have let

$$\mathscr{E}(f,g) \triangleq \int_\Omega \nabla f(x)^T a(x)\nabla g(x)\rho(dx)$$

denote the "Dirichlet Form." Let $\Omega \subset \mathbb{R}^n$ compact and open with smooth boundary. Let $\mathscr{L}^2(\bar{\Omega}, \rho)$ denote the Hilbert space of functions on $\bar{\Omega}$ which are square-integrable with respect to a continuous positive measure $\rho(dx) = e^{-U}dx$. Let $\mathcal{H}^1(\bar{\Omega}, \rho) = W^{1,2}(\bar{\Omega}, \rho) \subset \mathscr{L}^2(\bar{\Omega}, \rho)$ denote the corresponding once-weakly-differentiable Hilbert Sobolev space. Let $A, B \subset \Omega$, open, disjoint, with smooth boundary, and define $\text{cap}(A, \Omega \backslash B) \in \mathbb{R}$ as the minimizing value of the problem

$$\begin{aligned} \min_{u \in \mathcal{H}^1} \quad & \mathscr{E}(u, u) \\ \text{subject to} \quad & u(x) = 1, x \in A \\ & u(x) = 0, x \in B \end{aligned}$$

It is natural to consider an apparently different problem, where the equality boundary conditions are replaced with inequalities. Here we show that it is not possible to get lower than $\text{cap}(A, \Omega \backslash B)$ by such a relaxation.

Lemma 7. *Let $\tilde{h}$ satisfy $\tilde{h}(x) \geq 1$ on A and $\tilde{h}(x) \leq 0$ on B. Then $\mathscr{E}(\tilde{h}, \tilde{h}) \geq \text{cap}(A, \Omega \backslash B)$.*

Proof. Let $k = \texttt{clamp}(\tilde{h}, 0, 1)$, i.e.

$$k(x) = \begin{cases} \tilde{h}(x) & \tilde{h}(x) \in [0, 1] \\ 0 & \tilde{h}(x) \leq 0 \\ 1 & \tilde{h}(x) \geq 1 \end{cases}$$

Note that $k \in \mathcal{H}^1$ and satisfies the equality boundary conditions. Thus, by definition, $\text{cap}(A, \Omega \backslash B) \leq \mathscr{E}(k, k)$. This immediately yields our result:

$$\begin{aligned} \text{cap}(A, \Omega \backslash B) \leq \mathscr{E}(k, k) &= \int \|\sigma \nabla k\|^2 \rho(dx) \\ &= \int_{x:\ \tilde{h}(x) \in [0,1]} \|\sigma \nabla \tilde{h}\|^2 \rho(dx) \\ &\leq \int \|\sigma \nabla \tilde{h}\|^2 \rho(dx) = \mathscr{E}(\tilde{h}, \tilde{h}) \end{aligned}$$

□

Shell Method

The algorithm for estimating local hitting probabilities is outlined as follows:

Algorithm 1. *Estimating $h_{R,\tilde{R}^c}(x)$ for many values of x on a shell ∂S*

Input: *$R \subset S \subset \tilde{R} \subset \Omega$ and a stationary reversible diffusion process $\{X_t\}_{t\geq 0}$ in Ω with invariant measure $\mu = e^{-U(x)}\mathrm{d}x$. We also require a series of subsets*

$$R = S_0 \subset S_1 \subset \cdots \subset S_{m-1} \subset S_m = S \subset S_{m+1} \subset \cdots \subset S_n = \tilde{R}$$

which indicate a kind of reaction coordinate.

Output: *A collection of points $z_1, \cdots z_{N_p}$ on ∂S sampled from the invariant measure $\mu = e^{-U(x)}\mathrm{d}x$ restricted on ∂S, along with estimates of $h_{R,\tilde{R}^c}(z_i)$ for each point.*

1. *Discretize the space.*

   (a) *Generate an ensemble of samples $z_1, \ldots, z_{N_p}$ on ∂S according to the invariant measure $\mu = e^{-U(x)}\mathrm{d}x$ restricted to ∂S.*

   (b) *Evolve the ensemble on ∂S, by repeatedly sampling an initial location from the uniform distribution on $\{z_1, \ldots, z_{N_p}\}$ and carry out a local simulation following the dynamics of $\{X_t\}_{t\geq 0}$ until the trajectory hits either ∂S_{m-1} or ∂S_{m+1}. Record the hitting locations on ∂S_{m-1} and ∂S_{m+1} until we have N_p points on both ∂S_{m-1} and ∂S_{m+1}. In most cases, the process is more likely to hit one of S_{m-1}, S_{m+1} than the other, and we need to run more than $2N_p$ local simulations to get at least N_p samples on both shells. We store the results of the redundant local simulations for future estimation of transition probabilities.*

   (c) *Repeat the above process to sequentially evolve the ensembles on $\partial S_{m-1}, \ldots, \partial S_2$ and on $\partial S_{m+1}, \ldots, \partial S_{n-2}$, to get N_p samples on all of the intermediate shells $\partial S_1, \ldots, \partial S_{n-1}$. Store the results of the redundant local simulations for future estimation of transition probabilities.*

   (d) *For each one of the shells $\partial S_1, \ldots, \partial S_{n-1}$, cluster the N_p samples on that shell into N_b states. In our implementation, we use k-means, and represent the N_b states by the N_b centroids we get from the algorithm.*

The result of this step is a partitioning of each shell ∂S_i into N_b regions, representing an adaptive discretization of the shells. For a point on a shell ∂S_i, we identify its corresponding discrete state by finding the nearest centroid.

2. *Estimate the transition probabilities between these discrete states by running an additional N_s local simulations for each one of the N_b states on each shell. The result of this step is an estimate of the probability of transitioning from state k on ∂S_i to state l on ∂S_j, which we denote by $P_{k,l}^{(i,j)}$, where $k, l \in \{1, \ldots, N_b\}$ and $i, j \in \{1, \ldots, n-1\}$ with $|i - j| = 1$.*

3. *Use the transition probabilities to get an estimate of the hitting probabilities for the N_b states on ∂S. In line with related works on Markov state models,[11, 20, 27] we approximate the continuous dynamics using closed-form calculations from the discrete Markov chain we have developed in the previous two steps. In particular, we estimate overall hitting probabilities using the standard "one-step analysis." For any $k \in \{1, \ldots, N_b\}$ and $i \in \{1, \ldots, n-1\}$, let $u_k^{(i)}$ denote the probability of hitting $\partial R = \partial S_0$ before hitting $\partial \tilde{R} = \partial S_n$ if we start the discretized process at state k on ∂S_i. We can calculate our object of interest by solving the matrix difference equation*

$$u^{(i)} = P^{(i,i+1)}u^{(i+1)} + P^{(i,i-1)}u^{(i-1)}, i = 1, \ldots, n-1$$

with boundary conditions $u^{(0)} = \mathbf{1}, u^{(n)} = \mathbf{0}$, where $\mathbf{0}$ and $\mathbf{1}$ are vectors of all 0's and 1's. This gives the estimated hitting probability for each discrete state. We then estimate the hitting probability of each point z_i by

$$h_{R,\tilde{R}^c}(z_i) = u_k^{(m)}, z_i \in \text{state } k \text{ on } \partial S \tag{F1}$$

Details on Energy Function

For the energy function, we hand-designed two different kinds of landscape: random well energy, which we use for the region around target A, and random crater energy, which we use for the region around target B. The basic components of these energy functions are the

well component, given by

$$F_w(x|d_w, r) = -\frac{d_w}{r^4}(||x - x_A||_2^4 - 2r^2||x - x_A||_2^2) - d_w \tag{G1}$$

where d_w gives the depth of the well; the crater component, given by

$$F_c(x|d_c, h, r) = \frac{d_c}{3b^2r^4 - r^6}(2||x - x_B||_2^2 - 3(b^2 + r^2)||x - x_B||_2^4 + 6b^2r^2||x - x_B||_2^2) - d_c \tag{G2}$$

where d_c and h give the depth and the height of the crater, respectively, and

$$b^2 = -\frac{1}{3d}(-3d_cr^2 + C + \frac{\Delta_0}{C}) \tag{G3}$$

with

$$C = 3r^2\sqrt[3]{d_ch(d_c + \sqrt{d_c(d_c + h)})}$$
$$\Delta_0 = -9d_chr^4$$

and finally a random component, given by

$$F_r(x|\mu, \sigma) = \sum_{i=1}^{m}\prod_{j=1}^{d} exp(-\frac{(x_j - \mu_{ij})^2}{2\sigma_{ij}^2}) \tag{G4}$$

where $\mu = (\mu_{ij})_{m\times d}$ and $\sigma = (\sigma_{ij})_{m\times d}$, with $\mu_i = (\mu_{i1}, \cdots, \mu_{i,d}), i = 1, \cdots, m$ being the locations of m Gaussian random bumps in the region around the targets, and $\sigma_{ij}, i = 1, \cdots, m, j = 1, \cdots, d$ gives the corresponding standard deviations.

To make sure the energy function is continuous, and the different components of the energy function are balanced, we introduce a mollifier, given by

$$F_m(x|x_0, r) = exp(-\frac{r}{r - ||x - x_0||_2^{20}}) \tag{G5}$$

where $x_0 = x_A, r = r_{\dot{A}}$ or $x_0 = x_B, r = r_{\dot{B}}$, depending on which target we are working with, and a rescaling of the random component, which is given by $0.1 * d_w$ if we are perturbing the well component, and $0.1 * (d_c + h)$ if we are perturbing the crater component.

Intuitively, for the well component, we use a 4th order polynomial to get a well-like

energy landscape around the target that is continuous and differentiable at the boundary. Similarly, for the crater component, we use a 6th order polynomial to get a crater-like energy landscape around the target that is also continuous and differentiable at the boundary. For the random component, we are essentially placing a number of Gaussian bumps around the target. And for the mollifier, we are designing the function such that it's almost exactly 1 around the target, until it comes to the outer boundary, when it transitions smoothly and swiftly to 0. To summarize, given parameters d_w, d_c, h and random bumps μ_A, μ_B with $\mu_i^A \in \dot{A} \setminus A, i = 1, \cdots, m_A, \mu_i^B \in \dot{B} \setminus B, i = 1, \cdots, m_B$, and the corresponding standard deviations σ^A, σ^B with $\sigma_{ij}^A, i = 1, \cdots, m_A, j = 1, \cdots, d, \sigma_{ij}^B, i = 1, \cdots, m_B, j = 1, \cdots, d$, the energy function we used in the experiments is given by

$$F(x) = F_w(x|d_w, r_{\dot{A}}) + 0.1 \times d_w \times F_m(x|x_A, r_{\dot{A}}) + F_r(x|\mu^A, \sigma^A), \forall x \in \dot{A} \setminus A \tag{G6}$$

$$F(x) = F_c(x|d_c, h, r_{\dot{B}}) + 0.1 \times (d_c + h) \times F_m(x|x_B, r_{\dot{B}}) + F_r(x|\mu^B, \sigma^B), \forall x \in \dot{B} \setminus B \tag{G7}$$

In our actual experiments, we used

$$d_w = 10.0, d_c = 6.0, h = 1.0, \sigma_{ij}^A = \sigma_{k,l}^B = 0.01, \forall i, j, k, l$$

and

$$\mu^A = \begin{pmatrix} 0.512 & 0.583 & -0.013 & 0.013 & -0.001 \\ 0.464 & 0.575 & -0.001 & 0.019 & -0.014 \\ 0.503 & 0.611 & -0.012 & -0.024 & 0.023 \\ 0.5 & 0.601 & -0.024 & 0.034 & 0.011 \\ 0.486 & 0.586 & 0.006 & 0.01 & 0.001 \\ 0.489 & 0.588 & -0.017 & 0.002 & 0.027 \\ 0.493 & 0.585 & 0.015 & -0.001 & -0.032 \\ 0.516 & 0.596 & 0.027 & -0.026 & 0.022 \\ 0.514 & 0.624 & 0.01 & 0.01 & -0.002 \\ 0.5 & 0.605 & 0.017 & -0.016 & 0.004 \end{pmatrix}, \mu^B = \begin{pmatrix} -0.696 & -0.006 & 0.023 & -0.041 & 0.019 \\ -0.731 & 0.021 & -0.033 & -0.014 & 0.017 \\ -0.694 & -0.034 & -0.009 & 0.031 & 0.019 \\ -0.666 & -0.013 & 0.002 & 0.017 & 0.009 \\ -0.68 & 0.058 & 0.007 & -0.011 & -0.008 \\ -0.704 & -0.022 & 0.034 & 0.003 & 0.026 \\ -0.714 & -0.015 & 0.017 & 0.027 & 0.028 \\ -0.681 & 0.017 & -0.046 & -0.04 & -0.002 \\ -0.648 & -0.009 & 0.002 & -0.012 & -0.022 \\ -0.664 & -0.04 & 0.05 & -0.012 & -0.002 \end{pmatrix}$$

[1] NIST digital library of mathematical functions. `http://dlmf.nist.gov/`.

[2] D Aristoff, J Bello-Rivas, and R Elber. A mathematical framework for exact milestoning. *Multiscale Model. Simul.*, 14(1):301–322, January 2016.

[3] Árpád Baricz. Bounds for modified bessel functions of the first and second kinds. *Proceedings of the Edinburgh Mathematical Society*, 53(3):575–599, 2010.

[4] Eric B Baum. Intractable computations without local minima. *Phys. Rev. Lett.*, 57(21):2764–2767, November 1986.

[5] Juan M Bello-Rivas and Ron Elber. Exact milestoning. *J. Chem. Phys.*, 142(9):094102, March 2015.

[6] Nicholas H Bingham. Random walk on spheres. *Zeitschrift für Wahrscheinlichkeitstheorie und Verwandte Gebiete*, 22(3):169–192, 1972.

[7] Peter G Bolhuis, David Chandler, Christoph Dellago, and Phillip L Geissler. Transition path sampling: throwing ropes over rough mountain passes, in the dark. *Annu. Rev. Phys. Chem.*, 53:291–318, 2002.

[8] Zhen-Qing Chen. On reflecting diffusion processes and skorokhod decompositions. *Probability theory and related fields*, 94(3):281–315, 1993.

[9] Zhen-Qing Chen and Masatoshi Fukushima. *Symmetric Markov processes, time change, and boundary theory (LMS-35)*, volume 35. Princeton University Press, 2012.

[10] Alexei F Cheviakov, Michael J Ward, and Ronny Straube. An asymptotic analysis of the mean first passage time for narrow escape problems: Part ii: The sphere. *Multiscale Modeling & Simulation*, 8(3):836–870, 2010.

[11] John D Chodera and Frank Noé. Markov state models of biomolecular conformational dynamics. *Curr. Opin. Struct. Biol.*, 25:135–144, April 2014.

[12] Markus Christen and Wilfred F van Gunsteren. On searching in, sampling of, and dynamically moving through conformational space of biomolecular systems: A review. *J. Comput. Chem.*, 29(2):157–166, January 2008.

[13] Christoph Dellago, Peter G Bolhuis, Félix S Csajka, and David Chandler. Transition path sampling and the calculation of rate constants. *J. Chem. Phys.*, 108(5):1964–1977, February 1998.

[14] H.L. Dret and B. Lucquin. *Partial Differential Equations: Modeling, Analysis and Numerical Approximation.* International Series of Numerical Mathematics. Springer International Publishing, 2016.

[15] Weinan E. and Eric Vanden-Eijnden. Towards a theory of transition paths. *J. Stat. Phys.*, 123(3):503, May 2006.

[16] Weinan E and Eric Vanden-Eijnden. Transition-path theory and path-finding algorithms for the study of rare events. *Annu. Rev. Phys. Chem.*, 61:391–420, 2010.

[17] Daniel T Gillespie. The chemical langevin equation. *The Journal of Chemical Physics*, 113(1):297–306, 2000.

[18] D Holcman and Z Schuss. Escape through a small opening: receptor trafficking in a synaptic membrane. *Journal of Statistical Physics*, 117(5-6):975–1014, 2004.

[19] Adam Hospital, Josep Ramon Goñi, Modesto Orozco, and Josep L Gelpí. Molecular dynamics simulations: advances and applications. *Adv. Appl. Bioinform. Chem.*, 8:37–47, November 2015.

[20] Brooke E Husic and Vijay S Pande. Markov state models: From an art to a science. *J. Am. Chem. Soc.*, 140(7):2386–2396, February 2018.

[21] Huan Lei, Bruce Caswell, and George Em Karniadakis. Direct construction of mesoscopic models from microscopic simulations. *Physical Review E*, 81(2):026704, 2010.

[22] Gary M Lieberman. Mixed boundary value problems for elliptic and parabolic differential equations of second order. *Journal of Mathematical Analysis and Applications*, 113(2):422–440, 1986.

[23] Pierre-Louis Lions and Alain-Sol Sznitman. Stochastic differential equations with reflecting boundary conditions. *Communications on Pure and Applied Mathematics*, 37(4):511–537, 1984.

[24] Jackson Loper. Uniform ergodicity for brownian motion in a bounded convex set. *Journal of Theoretical Probability*, Jul 2018.

[25] J Machta. Strengths and weaknesses of parallel tempering. *Phys. Rev. E*, 80(5):056706, November 2009.

[26] Frank Noé, Dieter Krachtus, Jeremy C Smith, and Stefan Fischer. Transition networks for the comprehensive characterization of complex conformational change in proteins. *J. Chem. Theory Comput.*, 2(3):840–857, May 2006.

[27] Vijay S Pande, Kyle Beauchamp, and Gregory R Bowman. Everything you wanted to know about markov state models but were afraid to ask. *Methods*, 52(1):99–105, September 2010.

[28] D Pörschke. Elementary steps of base recognition and helix-coil transitions in nucleic acids. *Mol. Biol. Biochem. Biophys.*, 24:191–218, 1977.

[29] Harold A Scheraga, Mey Khalili, and Adam Liwo. Protein-folding dynamics: overview of molecular simulation techniques. *Annu. Rev. Phys. Chem.*, 58:57–83, 2007.

[30] Vassilios Sotiropoulos and Yiannis N Kaznessis. Analytical derivation of moment equations in stochastic chemical kinetics. *Chemical engineering science*, 66(3):268–277, 2011.

[31] Titus S van Erp and Peter G Bolhuis. Elaborating transition interface sampling methods. *J. Comput. Phys.*, 205(1):157–181, May 2005.

[32] David J Wales. Energy landscapes: calculating pathways and rates. *Int. Rev. Phys. Chem.*, 25(1-2):237–282, January 2006.

[33] J G Wendel. Hitting spheres with brownian motion. *Ann. Probab.*, 8(1):164–169, 1980.

[34] Anthony M A West, Ron Elber, and David Shalloway. Extending molecular dynamics time scales with milestoning: Example of complex kinetics in a solvated peptide. *J. Chem. Phys.*, 126(14):145104, April 2007.

[35] L T Wille. Intractable computations without local minima. *Phys. Rev. Lett.*, 59(3):372, July 1987.

[36] P Zhao, WB Zhang, and SJ Chen. Predicting secondary structural folding kinetics for nucleic acids. *Biophys J.*, 98(8):1617–1625, 2010.